NEANDC (E) - 302 U Vol. V
INDC (Ger) - 34/LN + Special

PROGRESS REPORT ON NUCLEAR DATA RESEARCH IN THE FEDERAL REPUBLIC OF GERMANY

for the Period April 1, 1988 to March 31, 1989

June 1989

Edited by
S. Cierjacks
Kernforschungszentrum Karlsruhe
Institut für Material- und Festkörperforschung II

NEANDC (E) - 302 U Vol. V
INDC (Ger) - 34/LN + Special

PROGRESS REPORT ON NUCLEAR DATA RESEARCH IN THE FEDERAL REPUBLIC OF GERMANY

for the Period April 1, 1988 to March 31, 1989

June 1989

Edited by
S. Cierjacks
Kernforschungszentrum Karlsruhe
Institut für Material- und Festkörperforschung II

This document contains information of a preliminary or private nature and should be used with discretion. Its contents may not be quoted, abstracted or transmitted to libraries without the express permission of the originator.

FOREWORD

This report has been prepared to promote the exchange of nuclear data research information between the Federal Republic of Germany and other member states of NEA and IAEA. It brings together progress reports from KfK Karlsruhe, KFA Jülich, GKSS Geesthacht, the universities of Hannover, Köln, Mainz, München and Stuttgart, as well as from PTB Braunschweig and FIZ Karlsruhe. As in previous years, the emphasis in the work reported here is on measurements, evaluation and compilation of application-oriented nuclear data, such as those relevant to fission and fusion reactor technologies, development of intense neutron sources, astrophysics research, cosmogenic and meteoritic investigations, production of medically important short-lived radioisotopes, etc.

Each contribution is presented under the laboratory heading where the work was done. When the work is relevant to requests in the World Request List for Nuclear Data, WRENDA 83/84 (INDC(SEC)-88/URSF), the corresponding request identification numbers are given in the headings of the respective contributions.

Karlsruhe, June 1989 S. Cierjacks

CONTENTS

Page

KERNFORSCHUNGSZENTRUM KARLSRUHE
INSTITUT FÜR KERNPHYSIK III

1. Measurement of the $^{22}Ne(n,\gamma)$ Cross Section at kT=25 KeV — 1
   H. Beer, G. Rupp, F. Voß, F. Käppeler

2. The Stellar Neutron Capture Cross Sections of $^{94,96}Zr$ — 3
   K.A. Toukan, F. Käppeler

3. First Measurements with the Karlsruhe 4π BaF_2 Detector — 4
   K. Wisshak, K. Guber, F. Käppeler, G. Rupp, H. Müller, F. Voß

KERNFORSCHUNGSZENTRUM KARLSRUHE
INSTITUT FÜR MATERIAL- UND FESTKÖRPERFORSCHUNG II

1. The Nuclear Data Base for Low-Activation Materials Development — 7
   K. Anderko, S. Cierjacks, Y. Hino

2. Element Activation by Sequential (x,n) Reactions in Fusion Reactor Materials — 7
   S. Cierjacks, Y. Hino

3. Study of a High-Performance Fast Neutron Source Based on the $H(t,n)^3He$ Reaction — 9
   S. Cierjacks, K. Ehrlich

KERNFORSCHUNGSZENTRUM KARLSRUHE
INSTITUT FÜR NEUTRONENPHYSIK UND REAKTORTECHNIK

1. Nuclear Data Evaluation — 12

1.1 Evaluation of Neutron Cross Sections for ^{238}U from 10 to 300 keV — 12
   F.H. Fröhner

page

INSTITUT FÜR CHEMIE (1): NUKLEARCHEMIE KERNFORSCHUNGSANLAGE JÜLICH

1. Neutron Data

1.1 First and Second Chance Proton Emission Reactions 15
S.M. Qaim, R. Wölfle

1.2 Study of (n,^{7}Be) Reactions 15
B. Scholten, S.M. Qaim, G. Stöcklin

1.3 Activation Cross Sections for Fusion Reactor Technology 16
R. Wölfle, M. Ibn Majah, N.I. Molla, S.M. Qaim, G. Stöcklin

2. Charged Particle Data

2.1 ^{7}Be-Emission in Proton Induced Reactions 17
B. Scholten, R. Wölfle, S.M. Qaim, G. Stöcklin

2.2 Cross Sections and Yields Relevant to Radioisotope Production 17
F. Tarkanyi, S.M. Qaim, G. Stöcklin

INSTITUT FÜR KERNPHYSIK KERNFORSCHUNGSANLAGE JÜLICH

1. (p,xn) Cross Sections and Yields at Medium Energies 21
W.B. Amian, R.C. Byrd, P. Cloth, D. Filges, C.A. Goulding
M.M. Meier, G.L. Morgan

2. Evaluation of a Neutron Cross Section Transport Library for Shielding Calculations up to 2.8 GeV 22
J. Moll, H. Schaal

3. Measurement and Validation Calculations of Double Differential Cross Sections for the Production of Light Charged Particles 24
K.-M. Koch, W. Amian, P. Dragovitsch, D. Filges, P. Cloth

page

4. Simulation of Galactic Cosmic Ray Interaction with Planetary Surfaces and its Application for Chemical Mapping 25
G. Dagge, P.Cloth, P. Dragovitsch, D. Filges, J. Brückner

5. Proton-Induced Production of Residual Nuclei in the Energy Range from 200 MeV to 5 GeV 27
P. Dragovitsch

GKSS-FORSCHUNGSZENTRUM GEESTHACHT GMBH
INSTITUT FÜR PHYSIK

14 MeV Neutron Activation Cross Sections 29
H.M. Agrawal, R. Pepelnik, Y. Tian, E. Bössow

ABTEILUNG NUKLEARCHEMIE
UNIVERSITÄT ZU KÖLN

ZENTRALEINRICHTUNG FÜR STRAHLENSCHUTZ
UNIVERSITÄT HANNOVER

1. Proton-Induced Spallation between 600 and 2600 MeV 31
B. Dittrich, U. Herpers, M. Lüpke, R. Michel

1.1 Production of Residual Nuclides by Proton-Induced Spallation between 600 MeV and 2600 MeV 31

1.2 Calculation of Production Cross Sections by Semiempirical Models and by Monte Carlo Modelling of the Intranuclear Cascade 36

INSTITUT FÜR KERNCHEMIE
UNIVERSITÄT MAINZ

Isomeric Ratios and Independent Yields of ^{134}I and ^{136}I in the Reactor Neutron Induced Fission of ^{232}Th 42
R. Hentzschel, H.O. Denschlag

page

FRM-REAKTORSTATION GARCHING, FACHBEREICH PHYSIK
TECHNISCHE UNIVERSITÄT MÜNCHEN

1. Scattering of Slow Neutrons on Thorium 45
W. Waschkowski, K. Knopf, L. Köster

INSTITUT FÜR KERNENERGETIK UND ENERGIESYSTEME
UNIVERSITÄT STUTTGART

1. Validation and Benchmark Testing of Evaluated Neutron Cross Sections for Hydrogen and Deuterium in the Liquid Phase 46
W. Bernnat, D. Emmendörfer, J. Keinert, M. Mattes

2. Pre-equilibrium Model Calculations with ALICE 49
M. Mattes, A. Sohn

3. Thermal Neutron Scattering Law Data in ENDF-6 Format 52
M. Mattes

PHYSIKALISCH-TECHNISCHE BUNDESANSTALT
BRAUNSCHWEIG

1. Neutron Data

1.1 Cross Section for the $^{27}Al(n,\alpha)$ and $^{24}Mg(n,p)$ Reactions 53
G. Börker, H. Klein, W. Mannhart, M. Wagner, G. Winkler

1.2 Measurement of the $^{54}Fe(n,\alpha)^{51}Cr$ Cross Section 54
W. Mannhart, G. Börker, G. Müller

1.3 Reaction Cross Section on Carbon for Energies from 11.5 MeV to 19 MeV 54
B. Antolkovic, G. Dietze, H. Klein

1.4 Measurement of Neutron Kerma Factors 56
H.J. Brede, P. Dahmen, H.G. Menzel, P. Pihet, U.J. Schrewe, H. Schuhmacher

page

2. Radionuclide Data

2.1 Photon Emission Probabilities 57
U. Schötzig

FACHINFORMATIONSZENTRUM KARLSRUHE

Status Report 60
H. Behrens, H.-W. Müller

1. Evaluated Nuclear Structure and Decay Data 60

2. Database GAMCAT 61

KERNFORSCHUNGSZENTRUM KARLSRUHE
INSTITUT FÜR KERNPHYSIK III

1. MEASUREMENT OF THE $^{22}Ne(n, \gamma)$ CROSS SECTION AT kT = 25 kEV*

H. Beer, G. Rupp, F. Voß, F. Käppeler

The $^{22}Ne(\alpha, n)$ reaction is considered as one of the primary neutron sources for the nucleosynthesis of the heavy elements. At the same time ^{22}Ne is effective as a neutron poison via the $^{22}Ne(n, \gamma)$ reaction. Therefore, its neutron capture cross section is of essential importance for the assessment of the neutron balance (1,2).

A $^{22}Ne(n,\gamma)$ measurement was performed using the activation technique. The $^{22}Ne(n,\gamma)^{23}Ne(38s)$ reaction is characterized by a clear signature. The radioactive nucleus ^{23}Ne decays in 32% of the cases via a 439 keV γ-ray line. With a high resolution germanium detector for activity counting this signature allowed us to accumulate the activation events into a sharp line distinct from the background countrate.

The activations were carried out at the Karlsruhe 3.75 MV van de Graaff accelerator. Using the $^{7}Li(p,n)^{7}Be$ reaction near the reaction threshold, a Maxwellian neutron spectrum with a thermal energy kT=25 keV can be obtained for the irradiations (3,4). The short half life of ^{23}Ne required the built-up of an experimental arrangement for fast cyclic activation in order to carry out irradiation and activity counting efficiently.

The ^{22}Ne capture cross section was determined relative to the well-known ^{197}Au cross section in two steps. This is necessary because of the special properties of neon as a noble gas. In the first step the $^{22}Ne(n, \gamma)^{23}Ne(38s)$ reaction was measured relative to five different Kr reactions :
$^{78}Kr(n, \gamma)\,^{79}Kr^{m}(50s)$, $^{78}Kr(n, \gamma)\,^{79}Kr(34.9h)$, $^{80}Kr(n, \gamma)\,^{81}Kr^{m}(13.3s)$, $^{84}Kr(n, \gamma)\,^{85}Kr^{m}(4.48h)$, $^{86}Kr(n, \gamma)\,^{87}Kr(76.3m)$. For these activations stainless steel spheres (20 mm diameter, 0,5 mm wall thickness) were filled with a mixture of enriched (99.9%) ^{22}Ne and natural Kr gas. In the second step, the same Kr reactions were measured relative to the $^{197}Au(n, \gamma)\,^{198}Au(2.69d)$ reaction. For this purpose Kr loaded zeolite was pressed to self-supporting tablets of 6 mm diameter and irradiated together with Au disks of the same diameter.

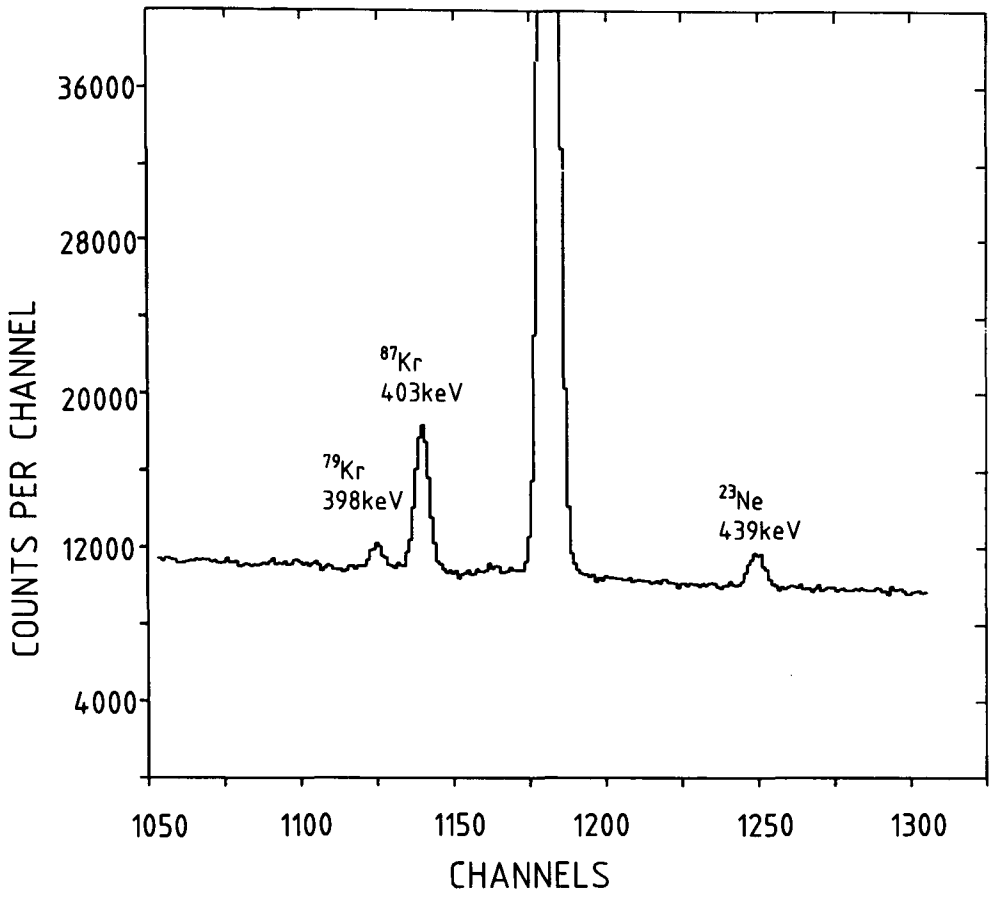

Fig. 1 A section of the accumulated data of one of the activations. The pressurized gas sample contained 250.36 mg ^{22}Ne and 210.88 mg natural Kr. Results on ^{22}Ne, ^{86}Kr and ^{78}Kr are shown. The capture events are determined from the intensities of the corresponding γ-ray lines of ^{23}Ne, ^{79}Kr and ^{78}Kr. The ^{23}Ne line contains 10,785, the ^{87}Kr line 41,096 and the ^{79}Kr line 5,245 counts. The strong line in the center is the 417 keV background line from the activation of ^{115}In by scattered neutrons.

The final analysis resulted in a Maxwellian averaged ^{22}Ne capture cross section of σ [^{22}Ne, kT = 25 keV] = (0.066 ± 0.005) mb; extrapolated to kT = 30 keV one obtains σ [^{22}Ne, kT = 30 keV] = (0.060 ± 0.005) mb. The quoted uncertainty was determined by quadratic error propagation from the following individual uncertainties : Statistics (^{22}Ne/Kr) 3.6%, Statistics (Kr/Au) 0.5%, Ge-detector efficiency 2%, Au cross section 1.5%, gas sample weight 5%, Kr weight in zeolite 2.5%, intensity per decay of ^{23}Ne line 3.04%, intensity per decay of ^{198}Au line 0.105%,γ-ray attenuation 1.5%, neutron multiple scattering < 1%.

(1) M. Busso, G. Picchio, R. Gallino, A. Chieffi, Ap. J. 326 (1988) 196
(2) N. Prantzos, M. Arnould, J.-P. Arcoragi, Ap. J. 315 (1987) 209
(3) H. Beer, F. Käppeler, Phys. Rev. C21 (1980) 534
(4) W. Ratynski, F. Käppeler, Phys. Rev. C37 (1988) 595

2. THE STELLAR NEUTRON CAPTURE CROSS SECTIONS OF $^{94,96}Zr$

K.A. Toukan* and F. Käppeler

The neutron capture cross sections of $^{94,96}Zr$ have been determined relative to that of gold by means of the activation method.The samples were irradiated in a quasi-stellar neutron spectrum for kT = 25 keV using the $^{7}Li(p, n)$ ^{7}Be reaction near threshold. Variation of the experimental conditions in different activations and the use of different samples allowed to reliably determine corrections and to evaluate systematic uncertainties. The resulting stellar cross sections are 28.6 ± 1.0 and 11.6 ± 0.4 mb for ^{94}Zr and ^{96}Zr, respectively. The respective uncertainties of about 4% are considerably lower than those of previous data. The new cross sections allowed for the first time to deduce the s-process neutron density from the branching at ^{95}Zr.

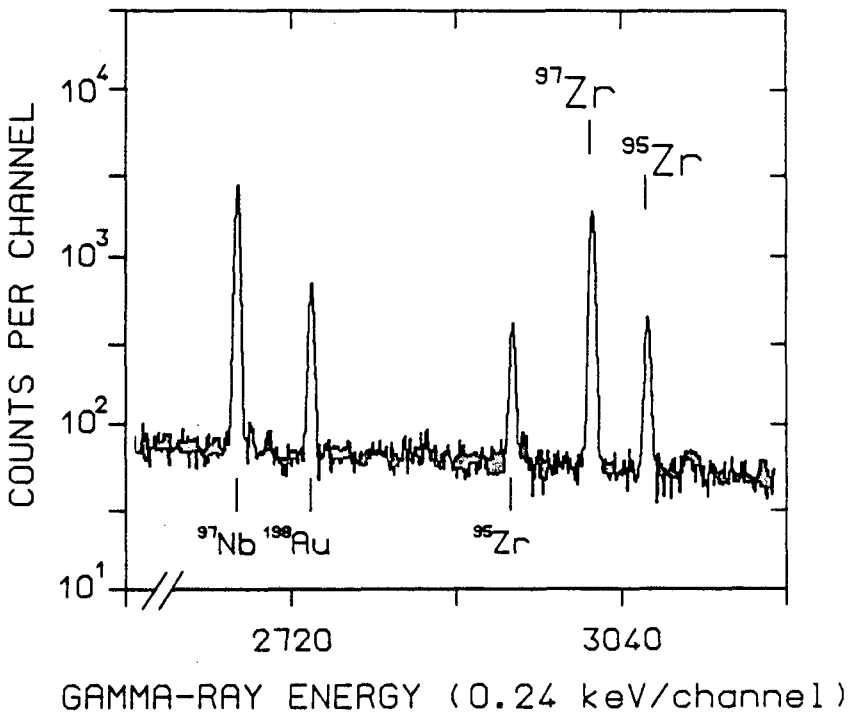

Fig. 1 Gamma-ray spectrum taken after activation of a zirconium foil sandwiched with a gold foil.

* On leave from University of Jordan, Amman, Jordan

3. FIRST MEASUREMENTS WITH THE KARLSRUHE 4π BaF_2 DETECTOR

K. Wisshak, K. Guber, F. Käppeler, G. Rupp, H. Müller, F. Voß

The Karlsruhe 4π BaF_2 detector has been completed by the end of 1987 (1, 2). Extensive test measurements with calibrated sources have been carried out to study the energy and time resolution as well as the efficiency for gamma-rays. During the first runs at the neutron beam, the individual background components were studied, and the neutron collimator was optimized. First cross section measurements have been performed on the monotopic elements niobium, tantalum and rhodium relative to gold as a standard.

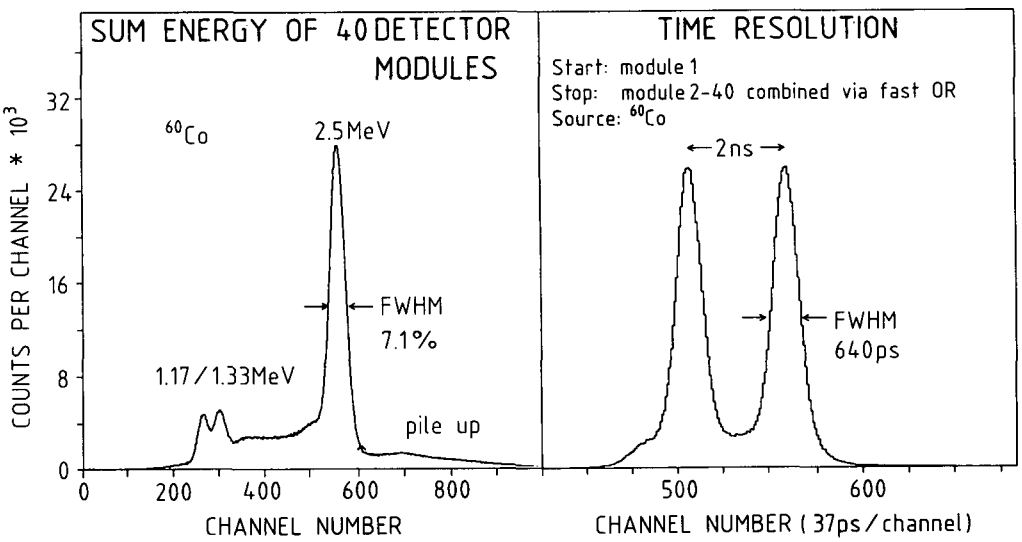

Fig. 1 Gamma-ray energy and time resolution of the total detector (with 40 out of 42 modules, ^{60}Co source).

Examples for the efficiency and resolution of the 4π detector are given in Fig. 1. These spectra were obtained with a ^{60}Co source and with 40 instead of 42 detector modules. Correspondingly, the solid angle covered by active crystals was only 95% of 4π, leading to a 5% intensity of the individual lines compared to 90% of the sum peak. The observed energy resolution of 7.1% is slightly worse than expected from the average resolution of the individual modules. This difference is mainly due to the limited resolution of the gain stabilization as the high voltage supply for the photomultipliers can only be changed in steps of 1 V. A time

resolution of 640 ps was measured for one reference module versus the rest of the detector, indicating a time resolution of 500 ps for the total detector. This value impressively illustrates the outstanding timing properties of BaF_2 crystals.

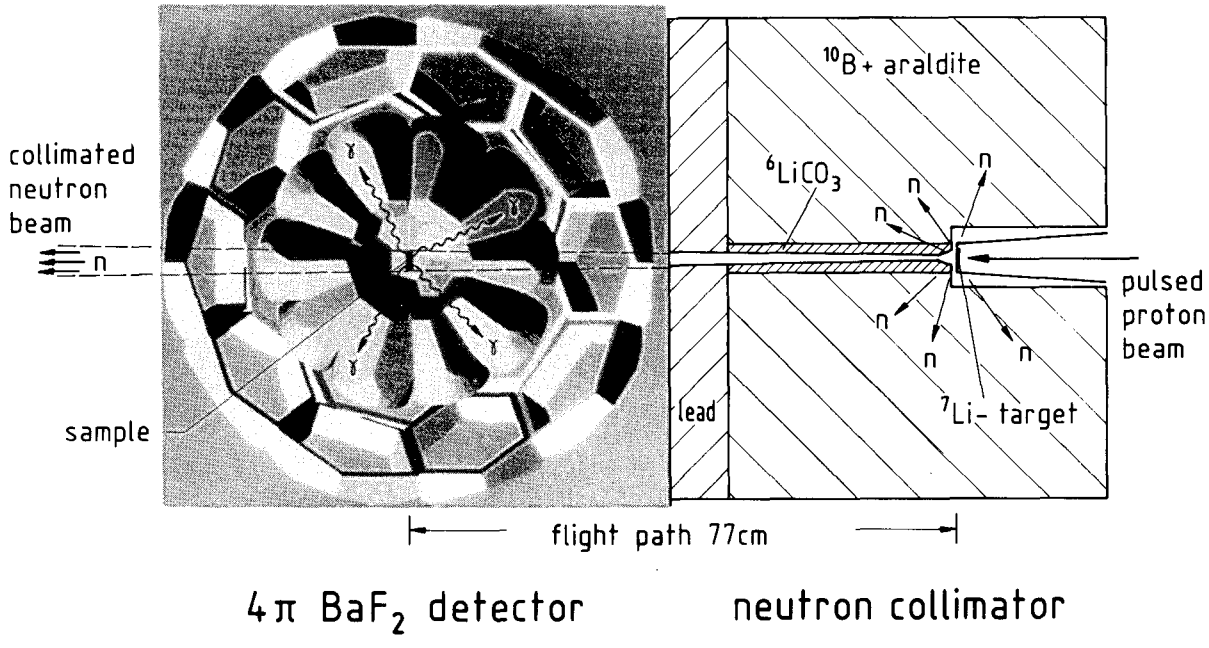

Fig. 2 Schematic setup for the determination of neutron capture cross sections in the energy range from 3 to 200 keV.

The experimental setup for the measurement of neutron capture cross sections is sketched in Fig. 2. The pulsed proton beam of the Van de Graaff accelerator (E_p = 1.97 MeV; rep. rate = 250 kHz; I_p = 2μA) falls on a metallic lithium target, producing a continuous neutron spectrum in the energy range from 3 to 200 keV via the $^7Li(p,n)^7Be$ reaction. A collimated neutron beam is produced by a carefully designed shield consisting mainly from boron, ^6Li-carbonate, and araldite. The neutron beam crosses the detector through holes in opposite crystals and is 25 mm in diameter at its centre. The neutron flight path was 77 cm.

During the measurements, two-dimensional spectra containing the sum energy of the gamma-ray cascade versus the time of flight were stored on-line. In addition, the same data were also recorded in list mode together with a 42 bit word per event indicating the particular modules that have contributed. This latter option provides for information on the gamma-ray multiplicity and for additional background suppression. Fig. 3 shows preliminary results for the multiplicity distribution of capture gamma cascades in a gold sample. The experimental points represent the number of modules that have fired in a

particular event, and are not yet corrected for detector-detector scattering, the limited solid angle of 95% of 4π, and the threshold in gamma-energy of ~60 keV for the individual modules. In view of all these effects, there is remarkably good agreement with a calculation by Reffo et al. (3).

In the cross section measurements, niobium, tantalum and rhodium samples with total masses between 1.6 and 0.5 g were used. The main background observed in these experiments is due to neutron scattering in air and to the radioactivity of the crystals. The first component will be suppressed introducing an evacuated tube for the neutron beam. The second component is reduced by a factor of two by replacing the seven crystals with the highest radium content. Therefore, in future experiments sample masses of less than 1 g should be sufficient, an important reduction as they will be carried out on isotopically

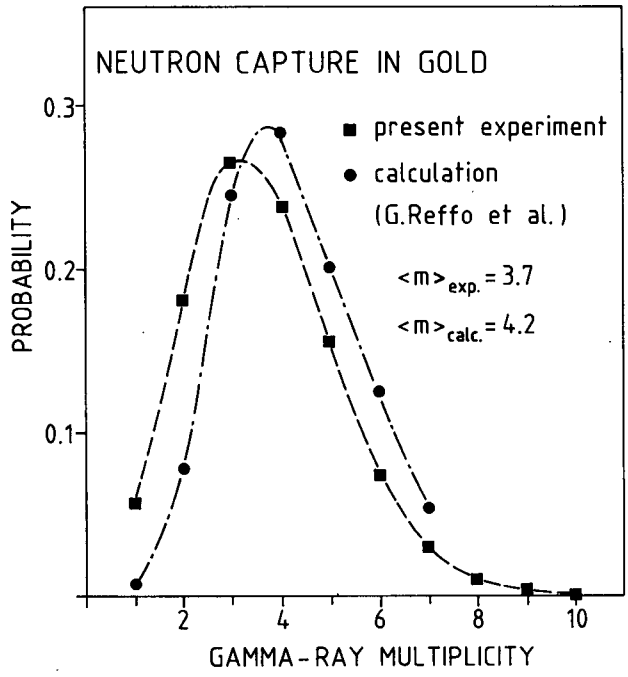

Fig. 4
Experimental distribution of cascade multiplicities following neutron capture in gold compared to a previous calculation.

enriched samples. In spite of the above backgrounds, a precision of ~1.5% could be achieved even in these first measurements (4).

(1) K. Wisshak, K. Guber, F. Käppeler, J. Krisch, H. Müller, G. Rupp, F. Voss, in Nuclear Data for Science and Technology (1988 Mito), ed. S. Igarasi (Saikon Publ. Comp., Tokyo 1988) p. 387

(2) K. Wisshak, F. Käppeler, F. Voss, K. Guber, 1988 Nuclear Science Symposium, IEEE Transactions on Nuclear Science, 36 (1989) 101

(3) G. Reffo, F. Fabbri, K. Wisshak, F. Käppeler, Nucl. Sci. Eng. 80 (1982) 630

(4) K. Wisshak et al. (1989), in preparation

KERNFORSCHUNGSZENTRUM KARLSRUHE
INSTITUT FÜR MATERIAL- UND FESTKÖRPERFORSCHUNG II

1. The Nuclear Data Base for Low-Activation Fusion Materials Development

K. Anderko, S. Cierjacks, Y. Hino

The development of low-activation materials (LAM) has been recently defined as one of the important tasks in DT fusion reactor development programs. Even though, in recent years there has been extensive work at various laboratories on the assessment of specific cross section and decay data libraries as well as on special processing codes, there are still large discrepancies in the various predictions of element activities and dose rates (e.g. for the potential alloying elements Ti, Ta, W, La, Hf, etc.). This is partly due to insufficient or discrepant nuclear data. But often an obvious reason is also an incomplete coverage of all kinematically allowed nuclear reaction channels for all target nuclei.

In support of current LAM programs within the European Fusion Technology Program [1], our institute has started work on activity, dose rate and afterheat calculations. Advantage was taken from the usage of the Harwell neutron cross section (UKACT1) and the decay data (UKDECAY2) libraries and the UK inventory code (FISPACT) [2]. First KfK-results obtained with the implemented UK code are shown in Fig. 1. It is the aim of our work to assess the accuracy of present predictions on element activations and dose rates for V-, Cr- and Fe-basis-alloy and their main tramp-impurity elements. Future work which is well coordinated with other laboratories aims at: i) A complete coverage of all possible reaction channels (including sequential (x,n) reactions; see Sec. 2). ii) Estimates of present data uncertainties and sensitivity studies. iii) Identification of critical data uncertainties and proposals for urgent data measurements.

2. Element Activation by Sequential (x,n) Reactions in Fusion Reactor Materials

S. Cierjacks, Y. Hino

In the past, activation calculations for materials irradiation in a fusion reactor spectrum have been restricted to neutron-induced reactions only. In principle, however, so-called "sequential (x,n) reactions" (in which charged particles (x) produced in a primary process A(n,x)B react in a

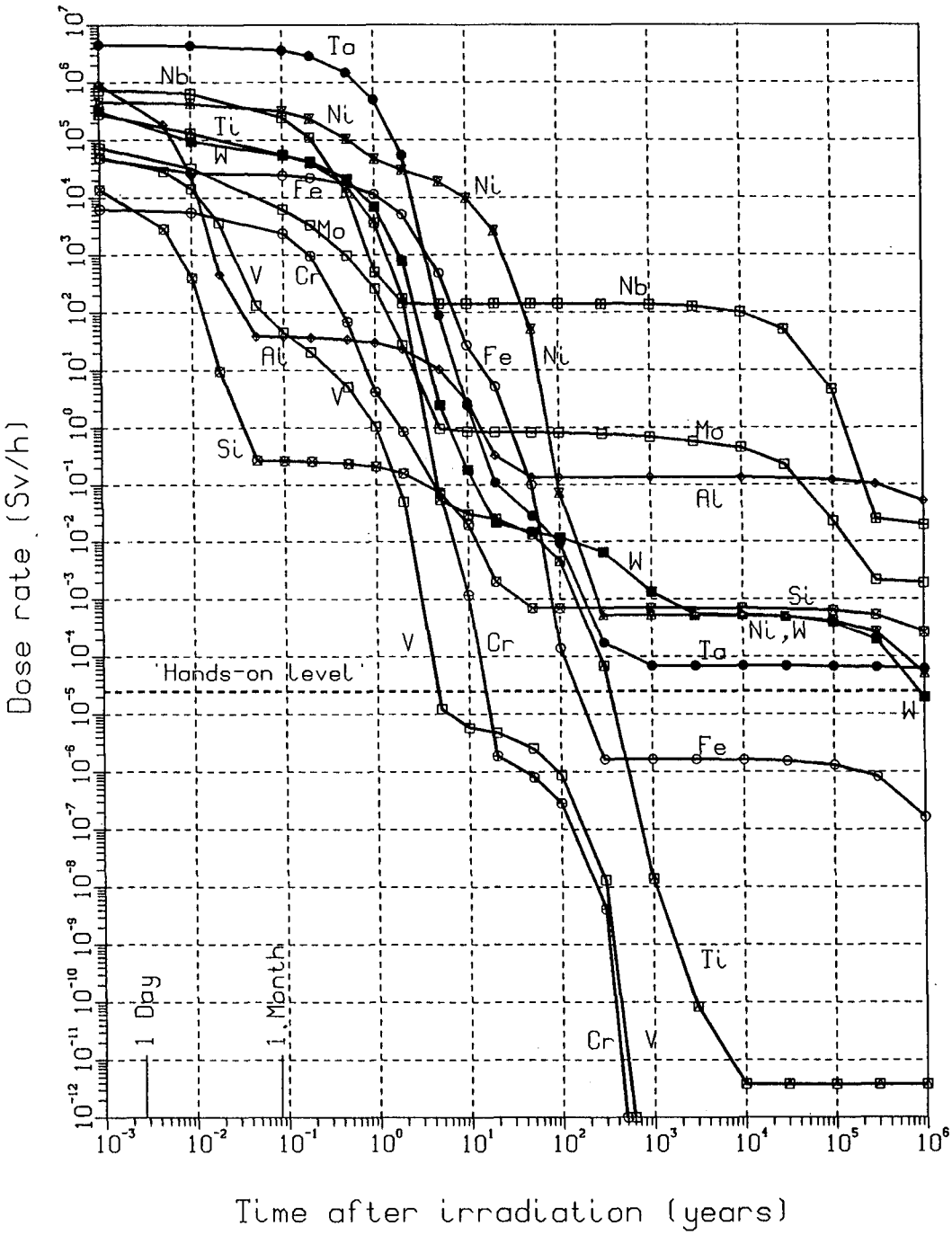

Fig. 1. KfK calculations [1] of time-dependent dose rates for 11 elements using the Harwell FISPACT code [2]. A wall loading of 5 MW m^{-2} for 2.5 years was assumed.

subsequent step by A(x,n)C with the target nucleus A) contribute additional activity, if C is a radionuclide. The effect of sequential (x,n) processes has been investigated for some medium weight target nuclei [3]. A typical result is shown in Table I.

Table I. Inventories and activities of product radionuclides from sequential (x,n) reactions on ^{56}Fe. Given results refer to a wall loading of 5 MW m^{-2} and an irradiation time of 2.5 years.

$Fe(n,xp) \rightarrow {}^{56}Fe(p,n)^{56}Co\ (T_{1/2} = 77.1\ d)$			
^{56}Co Inventory (2.5 y):	2.9×10^{17}	Nucl/kg	Uncertainty:
^{56}Co Activity (2.5 y):	3.1×10^{10}	Bq/kg	Factor 2
$Fe(n,xd) \rightarrow {}^{56}Fe(d,n)^{57}Co\ (T_{1/2} = 271.8\ d)$			
^{57}Co Inventory (2.5 y):	9.8×10^{16}	Nucl/kg	Uncertainty:
^{57}Co Activity (2.5 y):	2.9×10^{9}	Bq/kg	Factor 3
$Fe(n,x\alpha) \rightarrow {}^{56}Fe(\alpha,n)^{59}Ni\ (T_{1/2} = 7.5 \times 10^{4}\ y)$			
^{59}Ni Inventory (2.5 y):	1.4×10^{17}	Nucl/kg	Uncertainty:
^{59}Ni Activity (2.5 y):	4.0×10^{4}	Bq/kg	Factor 3

For the calculations we used measured differential neutron cross sections $d\sigma_n/dE_x$ [4], tabulated charged-particle stopping powers [5] and compiled energy-dependent (x,n) cross sections [6]. It can be seen from the table that the (x,n)-induced inventories and activities are many orders of magnitude higher than those used as present cut-off levels for neutron-induced reactions [2].

3. Study of a High-Performance Fast Neutron Source Based on the $H(t,n)^3He$ Reaction

S. Cierjacks, K. Ehrlich

A concept study for a novel neutron source has been performed which gives the main specifications for a facility involving a 21 MeV, 100-330 mA, triton beam incident on a thick hydrogen target [7]. Employing the H(t,n) source reaction (previously used as an intense monoenergetic source only) provides a source strength of 1.2×10^{16} and 3.9×10^{16} for 100 and 330 mA,

respectively. This source strength competes favourably with that of a deuterium-lithium source utilizing a 35 MeV deuteron beam of the same beam current incident on a lithium jet target. Two special, favourable characteristics of the tritium-hydrogen source for fusion materials testing are i) the kinematical collimation of neutrons into a narrow forward cone and ii) the cut-off of the neutron spectrum at 14.6 MeV. Due to difficulties with a pure hydrogen target at the MW power level, a water jet target has been considered instead. Target load calculations have been made, and spectrum and yield modifications connected with the oxygen content have been investigated. In addition to the special source study, a few general surveys on the present status and the future potential of neutron sources have been prepared [8-10].

References

[1] K. Anderko and S. Cierjacks; Difficulties with the nuclear data base for low-activation materials; Contribution to the IEA Workshop on Low-Activation Materials, Los Angeles, February 21-22, 1989.

[2] R. A. Forrest, D.A.J. Endacott and A. Khursheed; FISPACT - Program manual; Harwell Laboratory Report, AERE M 3655, April 1988; and R.A. Forrest and D.A.J. Endacott, Activation data for some elements relevant to fusion reactors; Harwell Laboratory Report, AERE R 13402, February 1989, and literature cited therein.

[3] S. Cierjacks and Y. Hino; Calculations of element activities and dose rates including neutron-induced and sequential (x,n) reactions; Kernforschungszentrum Karlsruhe Report, KfK-4523, to be published.

[4] S. M. Grimes, R.C. Haight, K.R. Alvar, H.H. Barschall, R.R. Borchers; Phys. Rev. C19 2127 (1979).

[5] C. Williamson and J.P. Boujot; Tables of range and rate of energy loss of charged particles of energy 0.5 to 150 MeV, Saclay Laboratory Report, 1962.

[6] K.A. Keller, J. Lange, H. Münzel and G. Pfennig; Anregungsfunktionen für Kernreaktionen mit geladenen Projektilen; ed. H. Schopper, in Landolt-Börnstein Vol. 5/1b, Springer Verlag, Berlin, 1973.

[7] S. Cierjacks and K. Ehrlich; Proposal for a high-intensity high-energy neutron source based on the $H(t,n)^3He$ reaction; Contribution

to the IEA Workshop on an International Fusion Materials Irradiation Facility (IFMIF), San Diego, February 14-17, 1989.

[8] S. Cierjacks and A.B. Smith; Neutron sources: Present practice and future potential; Proc. Int. Conference on Nuclear Data and Technology, Mito, Japan, May 30 - June 3, 1988, p. 325 ff.

[9] A. Möslang, S. Cierjacks and R. Lindau; Test of fusion reactor materials with cyclotrons and presentation of the Karslruhe Dual-Beam Facility; presented at the 12th Int. Conf. on Cyclotrons and their Applications, Berlin, to be published 1989.

[10] S. Cierjacks, coordinator; Special Issue of Nuclear Science and Engineering on "Neutron Sources for Fusion Technology and Fusion Materials Research"; to be published.

KERNFORSCHUNGSZENTRUM KARLSRUHE
INSTITUT FÜR NEUTRONENPHYSIK UND REAKTORTECHNIK

1. Nuclear Data Evaluation

1.1 Evaluation of Neutron Cross Sections for ^{238}U from 10 to 300 keV

F.H. Fröhner

The JEF-2 evaluation of neutron cross sections for ^{238}U in the unresolved resonance region (10 to 300 keV), relying heavily on the level-statistical model of compound-nuclear reactions (Hauser-Feshbach theory with GOE width fluctuations) has been completed [1]. Two major discrepancies could be clarified: (a) The photon strength functions, Γ_γ/D, deduced from resolved resonances on one hand and from resonance-averaged cross section data on the other, are now in agreement, after a reanalysis of resolved resonance parameters excluding all levels with doubtful spin and parity assignments yielded a mean level spacing of 22.8 eV. (b) An initial disagreement with a pointwise (model-free) ENDF/B-VI evaluation of the capture cross section has disappeared: The latest ENDF/B-VI standards evaluation of ^{238}U capture [2] agrees well over most of the range considered here, see Fig. 1. The final parameters for generation of cross section values with the Hauser-Feshbach code FITACS are given in Table 1. There is now perfect consistency of the parametrisation in the unresolved resonance range with the statistics of resolved levels, as well as with optical-model and giant-dipole resonance results at higher energies [3]. The calculated total cross sections agree to better than 1 % with a recent ANL evaluation [4].

References

[1] F.H. Fröhner, Proc. 1988 Int. Reactor Phys. Conf., Jackson Hole, ANS (1988), vol. III, p. 171
[2] W.P. Poenitz, private communication
[3] F.H. Fröhner, accepted for publ. by Nucl. Sci. Eng.
[4] A.B. Smith, private communication

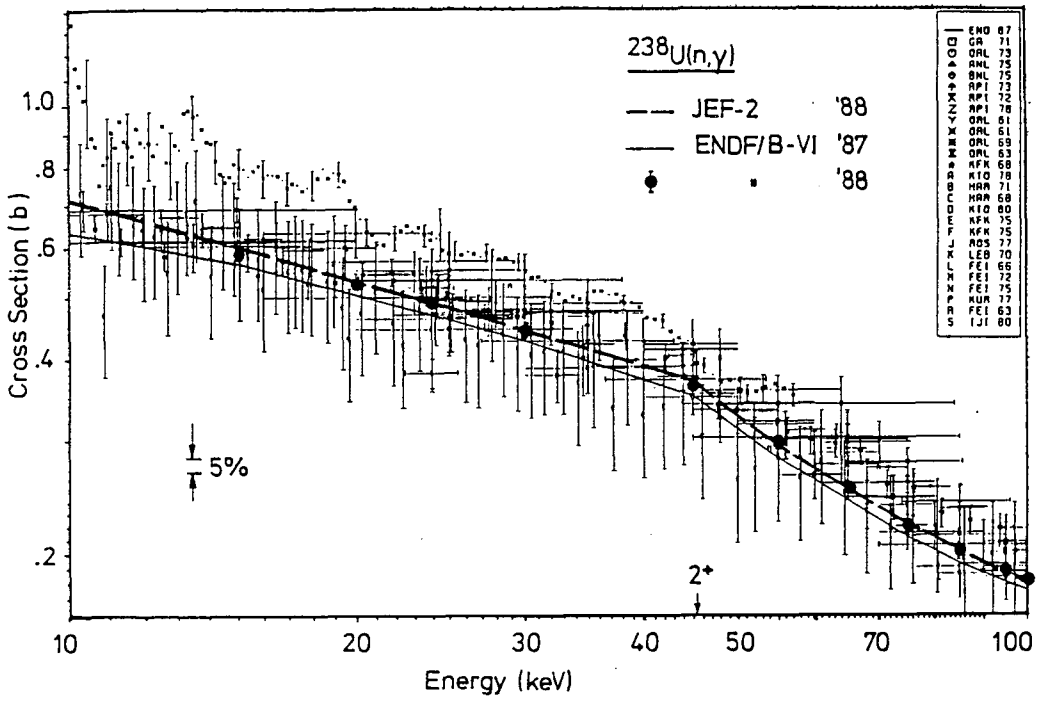

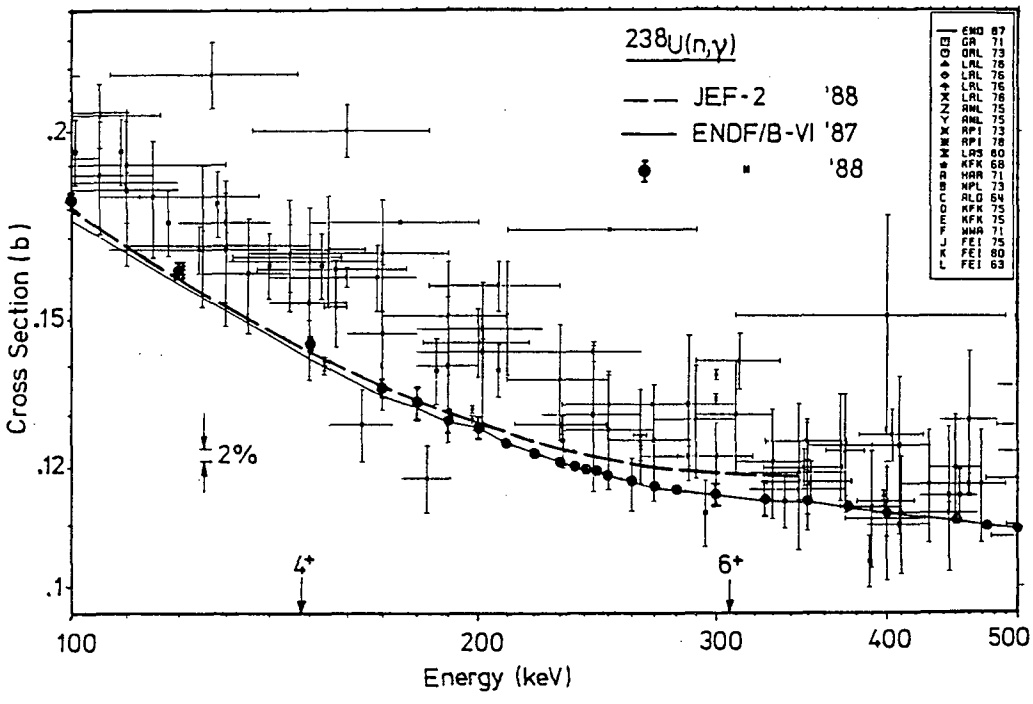

Fig. 1 - Capture cross section evaluations and data. Inelastic thresholds are indicated by spin-parity characteristics of residual levels. Experimental data (from NEA Data Bank) are indicative only: Many are uncorrected for multiple scattering and self-shielding and not renormalised to current reference cross sections.

Table 1: Average Resonance Parameters (for E = 0) Used to Generate JEF-2 Data between 10 and 300 keV

Orbital Angular Momentum ($\hbar$)	Neutron Strength Function (10^{-4})	Distant Level Parameter	Average Radiation Width (meV)	Mean Level Spacing (eV)	Effective Nuclear Radius
0	0.98	-0.12	22.6	23.0	9.43
1	2.01	0.19	22.7		
2	1.24	-0.06	22.6		
3	2.00	0.18	22.7		

INSTITUT FÜR CHEMIE (1): NUKLEARCHEMIE
KERNFORSCHUNGSANLAGE JÜLICH

1. Neutron Data

1.1 First and Second Chance Proton Emission Reactions

S.M. Qaim, R. Wölfle

Excitation functions were measured radiochemically for the $^{92}Mo(n,p)^{92m}Nb$ and $^{92}Mo(n,n'p+pn+d)^{91m}Nb$ reactions in the incident neutron energy ranges of 9 to 10.6 and 12.6 to 14.4 MeV. Use was made of high-resolution γ-ray spectroscopy in the former case and X-ray spectroscopy in the latter. For both the reactions statistical model calculations taking into account precompound effects were performed in collaboration with IRK Wien (B. Strohmaier). The results for the $^{92}Mo(n,n'p+pn+d)^{91m}Nb$ reaction are shown in Fig. 1. The model calculation gives the magnitudes of the (n,n'p) and (n,pn) processes, the (n,d) contribution being negligibly small. At all incident neutron energies the (n,n'p) channel is much stronger than the (n,pn) channel. A comparison of the (n,p) and (n,n'p) cross section data suggested that the second chance proton emission is significant for neutron energies above 11 MeV; between 13 and 14 MeV it is comparable to the first chance proton emission.

1.2 Study of (n,^{7}Be) Reactions

B. Scholten, S.M. Qaim, G. Stöcklin

In connection with our radiochemical studies on complex particle emission in fast neutron induced reactions [cf. 1,2], we initiated investigations on the emission of ^{7}Be. Several elements (and compounds) were irradiated with 53 MeV d (Be) breakup neutrons and the neutron flux density was determined via the $^{27}Al(n,\alpha)^{24}Na$ reaction. The irradiated samples were processed chemically and ^{7}Be was separated. Its activity was then determined via γ-ray spectroscopy. Preliminary results on V, Mn, As, Nb and Au show that the (n,^{7}Be) cross section is very low (μb region). Detailed investigations are in progress.

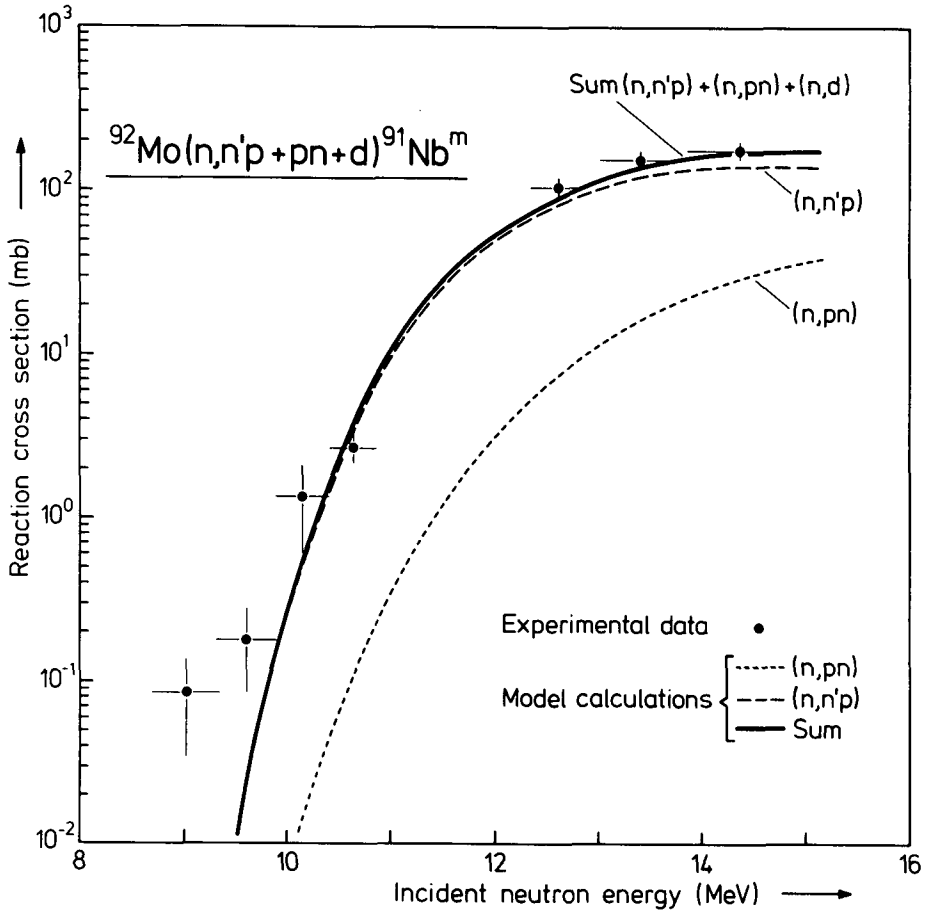

Fig. 1 Excitation function of the ^{92}Mo(n,n'p+pn+d)^{91m}Nb process. The results of model calculations are given as curves. The calculated (n,d) contribution is negligibly small and is not shown.

1.3 Activation Cross Sections for Fusion Reactor Technology

R. Wölfle, M. Ibn Majah, N.I. Molla, S.M. Qaim, G. Stöcklin
(Relevant to request identification numbers: 722148F, 724041F, 724042F, 724055F, 724056F, 742127R, 812002F, 812003F, 861175F, 873007R)

In continuation of our radiochemical measurements on activation products [3,4], we completed systematic studies on the ^{90}Zr(n,p)^{90m,g}Y, ^{91}Zr(n,p)^{91m,g}Y, ^{91}Zr(n,p)^{92}Y, ^{90}Zr(n,α)^{87m}Sr, ^{94}Zr(n,α)^{91}Sr and ^{96}Zr(n,2n)^{95}Zr reactions from threshold up to 10.6 MeV. Zirconium is an important reactor material but the data base up to 13 MeV was very weak. Our results should provide some useful information in the investigated energy region.

Titanium is a potential constituent of first wall materials of a fusion reactor. Measurements of (n,p) and (n,α) reactions on several isotopes of titanium are under way in the energy range of 5 to 10.6 MeV. Of special interest is the $^{48}Ti(n,\alpha)^{45}Ca$ ($T_{\frac{1}{2}}$ = 163 d; E_{β^-} = 0.3 MeV) reaction which can be measured only radiochemically using low-level β^--counting. First results show that its cross section at 10 MeV is a few mb.

Excitation function measurements on the reactions $^{92}Mo(n,\alpha)^{89}Zr$, $^{95}Mo(n,p)^{95m,g}Nb$, $^{96}Mo(n,p)^{96}Nb$, $^{98}Mo(n,\alpha)^{95}Zr$ and $^{100}Mo(n,\alpha)^{97}Zr$ in the neutron energy range of 12.5 to 20 MeV in collaboration with CBNM Geel (H. Liskien, R. Widera) were completed [5].

The status of experimental data relevant to fusion reactor technology was reviewed [6].

2. Charged Particle Data

2.1 ^{7}Be-Emission in Proton Induced Reactions

B. Scholten, R. Wölfle, S.M. Qaim, G. Stöcklin

^{7}Be emission in high energy proton induced spallation of a few nuclei has been reported. For light mass nuclei some information is also available in the low energy region. We investigated for the first time the excitation functions of (p,^{7}Be) reactions on ^{51}V, ^{93}Nb and ^{197}Au in the proton energy range from threshold to 105 MeV. The stacked foil technique in combination with radiochemical separations and γ-ray spectroscopy was applied. The cross section at the maximum energy used amounts to < 1 mb. Cross sections were also measured for ^{7}Be-emission in the spallation of V, Nb and Au with 800, 1200 and 2600 MeV protons. Values of a few mb were obtained.

2.2 Cross Sections and Yields Relevant to Radioisotope Production

F. Tárkányi, S.M. Qaim, G. Stöcklin

Continuing our studies [cf. 7-12] on the production of medically important short-lived β^+-emitting and single photon emitting radioisotopes we measured excitation functions and yields for the formation of ^{82}Sr and

^{123}I. Cross section measurements relevant to the production of ^{82}Sr (parent of β^+ emitting 1.2 min ^{82}Rb) via the $^{nat}Kr(^3He,xn)^{82}Sr$ and $^{nat}Kr(\alpha,xn)^{82}Sr$ processes, reported earlier [11,12], were extended to cover the higher energy region up to 120 MeV [13]. The α-particle induced process over the energy range of E_α = 120 → 20 MeV was found to be especially suitable. The calculated thick target yield of ^{82}Sr amounts to 52 μCi (1920 KBq)/μAh and the $^{85}Sr/^{82}Sr$ ratio 1.24. This yield value is only by a factor of 2 smaller than that of the presently used spallation process.

In recent years ^{123}I has been produced in high yield and high purity via the $^{124}Xe(p,x)^{123}I$-process on highly enriched ^{124}Xe. The nuclear data information available on this process, however, has been relatively scanty. We measured differential yields of ^{123}I as a function of energy in proton and deuteron bombardment of natural Xe gas [14]. The energy range covered in the case of protons was 17 to 43 MeV and for deuterons 22 to 53 MeV. The results for proton induced reactions are shown in Fig. 2. The optimum energy range for the production of ^{123}I is E_p = 30 → 24 MeV and the expected yield (assuming 99.8 % enriched ^{124}Xe) is 11 mCi/μAh. Cross section measurements using ^{124}Xe of various enrichments are in progress.

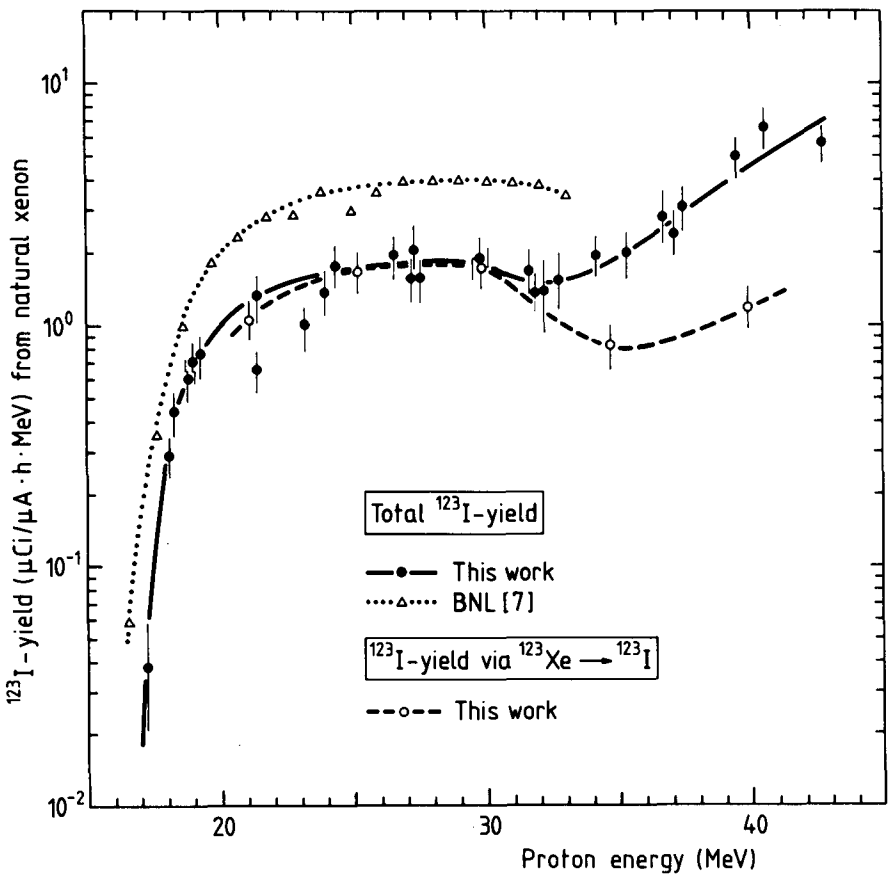

Fig. 2 Differential yield of ^{123}I at 6.6 h after EOB as a function of proton energy on natural xenon.

References

[1] A. Suhaimi, R. Wölfle, S.M. Qaim, P. Warwick, G. Stöcklin: Measurement of $^{14}N(n,t)^{12}C$ reaction cross section in the energy range of 5.0 to 10.6 MeV, Radiochimica Acta 43 (1988) 133

[2] S.M. Qaim, A. Suhaimi, R. Wölfle, G. Stöcklin: Measurement of (n,t) cross sections on light nuclei, Proc. Int. Conf. on Nuclear Data for Science and Technology, Mito, Japan, May/ June 1988, JAERI (1988) p. 225

[3] A. Mannan, S.M. Qaim: Activation cross section and isomeric cross section ratio for the $^{93}Nb(n,\alpha)^{90m,g}Y$ reaction, Phys. Rev. C38 (1988) 630

[4] R. Wölfle, A. Mannan, S.M. Qaim, H. Liskien, R. Widera: Excitation functions of $^{93}Nb(n,2n)^{92m}Nb$, $^{93}Nb(n,\alpha)^{90m,g}Y$, $^{139}La(n,\alpha)^{136}Cs$ and $^{181}Ta(n,p)^{181}Hf$ reactions in the energy range of 12.5 to 19.6 MeV, Appl. Radiat. Isotopes 39 (1988) 407

[5] H. Liskien, R. Wölfle, R. Widera, S.M. Qaim: Excitation functions of (n,p) and (n,α) reactions on molybdenum isotopes, Appl. Radiat. Isotopes, in press

[6] S.M. Qaim: Recent developments in cross-section measurements for fusion reactors, Proc. Int. Conf. on Nuclear Data for Science and Technology, Mito, Japan, May/June 1988, JAERI, (1988) p. 179

[7] S.M. Qaim, M.S. Sutisna, H. Ollig: Production of ^{38}K via the $^{35}Cl(\alpha,n)$-process at a compact cyclotron, Appl. Radiat. Isotopes 39 (1988) 479

[8] A. Mushtaq, S.M. Qaim, G. Stöcklin: Production of ^{73}Se via (p,3n) and (d,4n) reactions on arsenic, Appl. Radiat. Isotopes 39 (1988) 1085

[9] S.M. Qaim, F. Tárkányi, A. Mushtaq, G. Stöcklin: Excitation functions for the production of positron emitting radionuclides $^{82}Sr(^{82}Rb)$ and ^{73}Se, Proc. Int. Conf. on Nuclear Data for Science and Technology, Mito, Japan, May/June 1988, JAERI (1988) p. 1083

[10] B. Scholten, S.M. Qaim, G. Stöcklin: Excitation functions of proton induced nuclear reactions on natural tellurium and enriched ^{123}Te: Production of ^{123}I via the $^{123}Te(p,n)^{123}I$-process at a low-energy cyclotron, Appl. Radiat. Isotopes 40 (1989) 127

[11] F. Tárkányi, S.M. Qaim, G. Stöcklin: Excitation functions of ^{3}He- and α-particle induced nuclear reactions on natural krypton: Production of ^{82}Sr at a compact cyclotron, Appl. Radiat. Isotopes 39 (1988) 135

[12] F. Tárkányi, S.M. Qaim, G. Stöcklin: Excitation functions of ^{3}He-particle induced nuclear reactions on enriched ^{82}Kr and ^{83}Kr, Radiochimica Acta 43 (1988) 185

[13] F. Tárkányi, S.M. Qaim, G. Stöcklin: Excitation functions of high-energy ^{3}He- and α-particle induced nuclear reactions on natural krypton with special reference to the production of ^{82}Sr, Appl. Radiat. Isotopes, in press

[14] F. Tárkányi, Z. Kovács, S.M. Qaim, G. Stöcklin: Differential production yields of ^{123}I in proton and deuteron induced reactions on natural xenon, Radiochimica Acta, in press

INSTITUT FÜR KERNPHYSIK, ARBEITSGRUPPE STRAHLUNGSTRANSPORT KERNFORSCHUNGSANLAGE JÜLICH

1. (p,xn) Cross Sections and Yields at Medium Energies

W.B. Amian, R.C. Byrd*, P. Cloth, D. Filges, C.A. Goulding*, M.M. Meier*, G.L. Morgan*

Neutron production cross sections and yield data for reactions initiated by medium energy protons were measured at the Los Alamos WNR facility. These data provide benchmarks for INCE codes like HETC that are widely used to predict secondary particle spectra produced in the interactions of hadrons with matter.

The time-of-flight technique was used to determine the neutron energy spectra and to identify and discriminate against backgrounds. Five flight paths with detector stations were operational: 7.5° at 50 m, 30° at 30 m, 60° at 60 m, 120° at 25 m, and 150° at 30 m. The collimation scheme was flexible enough to allow both fields of view for thin targets (<3.5 MeV) and stopping-length targets. Shielding was a minimum of 37 dose-attenuation lengths. The detectors were cylindrical plastic scintillators. Their efficiencies were determined at several biases using light-ion reactions as neutron sources of known intensity for neutron energies below 35 MeV and the ^{7}Li(p,n) ^{7}Be (g.s. +0.43 MeV) reaction at zero degrees between 30 and 200 MeV. The proton charge normalization was against the ^{27}Al(p,x) ^{22}Na cross section. Data were acquired at three different biases simultaneously using fast CAMAC electronics. Both target-out backgrounds and shadowbar corrections were applied before obtaining the final cross sections or yields.

So far data have been analyzed for experiments at incident proton energies of 113 MeV and 256 MeV. At 113 MeV targets of elemental beryllium, carbon, aluminum, iron, and depleted uranium were studied both for thin and stopping length targets. Additional cross section measurements were done for oxygen, tungsten, and lead. At 256 MeV yields and cross sections for elemental beryllium, carbon, aluminum, and iron were measured. Cross sections for oxygen, lead and depleted uranium were obtained, as well. Comparisons of the experimental data with INCE calculations, using the KFA version of HETC /1/ are underway.

Reference

/1/ P. Cloth, D. Filges, R.D. Neef, Ch. Reul, G. Sterzenbach, T.W. Armstrong, B.L. Colborn, B. Anders, H. Brückmann HERMES, A Monte Carlo Program System for Beam-Materials Interaction Studies, Jül-2203, May 1988

*Los Alamos National Laboratory / USA

2. Evaluation of a neutron cross section transport library for shielding calculations upto 2.8 GeV

J.Moll, H.Schaal*

In 1983 the cross-section-libraries HILO /1/ and LASL /2/ have been combined to the ANISN-formated LAHI-library /3/ to get a wide ranged cross-section-data-base especially for deep penetration calculations. LAHI included neutron-production-cross-sections from 10^{-10} MeV up to 800 MeV (53 groups) and γ-production-cross-sections between 10^{-2} MeV and 14 MeV (21 groups) as Legendre-coefficients of order P0-P3. In connection with the cooler-synchrotron-project (COSY) at KFA an expansion of the LAHI-library upto COSY related energies (2.8 GeV) seemed to be useful to perform shielding calculations at that facility. It was decided to create 9 additional energy groups for each of the 8 LAHI elements (Tab. 1).

P–Order	Group Number	Elements							
		H	C	O	Si	Al	Fe	Pb	W
P–0	1	σ abs. σ trans. Coeffic.	....	....	....	....			
	2 ⋮ 86	σ abs. σ trans. Coeffic.	....	....					
P–1	1 ⋮ 86	....	.....						
P–2	....								
P–3	....								

Tab. 1: Global structure of the LAHI-library

Cross section data were calculated by use of the Intra-Nuclear-Cascade-Evaporation model (INCE) implemented in the HETC-KFA2-code of the HERMES system /4/. A special input-design (Thin-Target-Setup) yields neutron-production-cross-sections including

*KFA-ISI

multiplicities. The demand of high energy- and angle- resolution on the one hand and sufficient statstics on the other hand required a minimum of 30000 calculated events for each problem. The incident neutron energy was assumed to be equally distributed over the respective energy group. The method of calculation was tested in lower energy ranges and showed quite good agreement with existing LAHI-data. *Fig. 1* shows the behaviour of the transport-cross-section over the whole energy range and *Fig. 1* points out the high energy region.

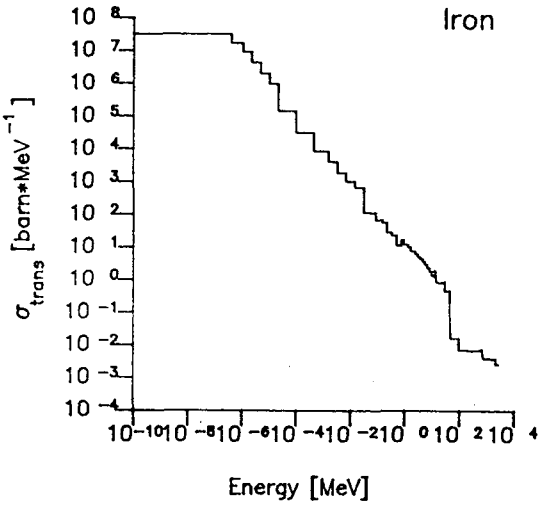

Fig. 1: σ_{trans} for element iron over all energies

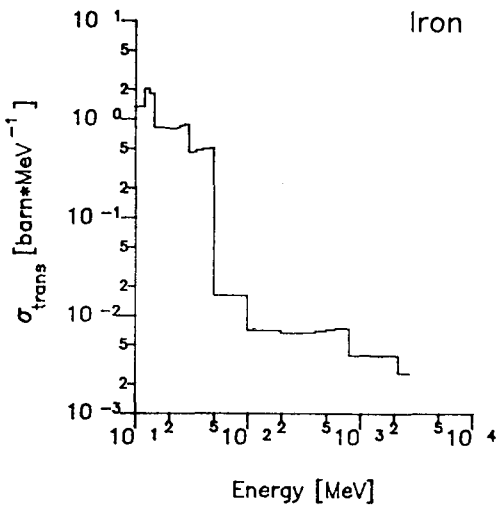

Fig. 2: σ_{trans} for element iron in high energy region

The present results are in good consistence within existing data and have yet been useful in COSY shielding calculations.

References

/1/ R.G. Alsmiller,Jr., J. Barish: *Neutron-Photon-Multigroup Cross Section for Neutron Energies < 400MeV*, **ORNL/TM-7818**, Oak Ridge (1981)

/2/ W.B. Wilson: *Nuclear Data Development and Shield Design for Neutrons Below 60MeV*, **LA-7159-T**, Los Alamos (1978)

/3/ H.Schaal et al.: *Combination of the high energy libraries LASL and HILO as LAHI-library for deep penetration calculations*, **SPA/04/83**, Institut für Reaktorentwicklung, KFA-Jülich (1983)

/4/ P. Cloth, D. Filges, R.D. Neef, G. Sterzenbach, Ch. Reul, T.W. Armstrong, B.L. Colborn, B. Anders, H. Brückmann: *HERMES. A Monte Carlo Program System for Beam-Materials Interaction Studies* , **Jül-2203**, Institut für Reaktorentwicklung, KFA-Jülich, May 1988

3. Measurement and Validation Calculations of Double Differential Cross Sections for the Production of Light Charged Particles

K.-M. Koch, W. Amian, P.Dragovitsch D. Filges and P. Cloth

The low current target area (WNR) at the Los Alamos Meson Physics Facility (Lampf) has been used for the determination of light charged particle ($A < 10$) production. The particles were generated on thin targets (C 82 $\mu g/cm^2$, Al 200 $\mu g/cm^2$, Cu 1000 $\mu g/cm^2$ and Pb 320 $\mu g/cm^2$) and viewed by a 12.3 m long time-of-flight vacuum telescope under 38 degree. Four standard transmission Si surface barrier detectors (thickness 150, 150,1500 and 1500 μm) and one Plastic Pilot B scintillator (thickness 50 mm) were employed in a sandwich set-up to detect the charged particle spectra. A ΔE, E and time-of-flight based analysis algorithm (Table-look-up procedure) made it possible to seperate protons (2 - 65 MeV), deuterons (3 - 100 MeV), tritons (5 - 120 MeV), He-3 particles (5 - 220 MeV), He-4 particles (5 - 220 MeV), and particles with masses 6,7,8,9 (4 - 30 MeV) with an energy resolution better than 2.5 %. The data have been reduced to double differential cross sections, with special consideration on target self absorption, in and out scattering effects, and background corrections. The overall accuracy of the measurement is primary due to low counting statistics, absolute proton amount estimation and target thickness variations from 18 to 29 %. The results are in good agreement with other data /1-3/, and show systematic non-equilibrium particle flux- target mass relations. Details of the measured data and comparitive calculations are given in Ref. /4/.

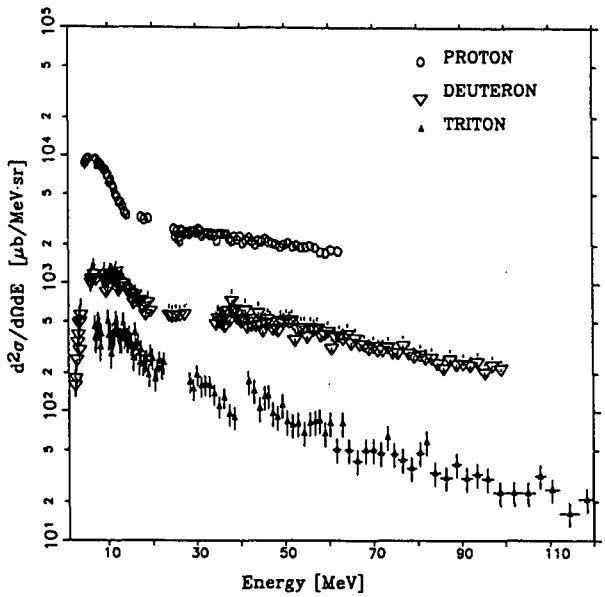

Fig. 1: Cross section for proton, deuteron and triton production at 38 deg from copper bombarded with 800 MeV protons

References

/1/ S. Nagamiya Phys. Rev.C Vol 24.971(1981)
/2/ S.C. Luckstead Los Alamos Report LA-7464-T(1978)
/3/ D.R. Cochran Phys. Rev. D Vol 6,3085(1972)
/4/ K.-M. Koch, Thesis, RWTH Aachen, in print

4. Simulation of Galactic Cosmic Ray Interaction with Planetary Surfaces and its Application for Chemical Mapping

G. Dagge, P. Cloth, P. Dragovitsch, D. Filges
and
J. Brückner (Max-Planck-Institut f. Chemie, Mainz)

For developing an analysis method for martian gamma ray spectra, which are caused by incident galactic cosmic rays (GCR), the Monte Carlo code system HERMES (1) is used for parameter studies concerning chemical composition and layered surface structures. The γ-spectrum as a characteristical fingerprint of the surface may be detected by an orbiting spacecraft. A validation of the code system was performed by simulating a 2π-GCR-irradiation of the lunar surface. The resulting depth profile of the neutron density was in excellent agreement (Fig. 1) with experimental data (2). The Cd ratio giving information on the energy distribution could be reproduced as well (Tab. I).

Table I: Cd-ratio $\frac{\text{total neutron density } \rho}{\rho<0.5\text{eV}}$ as a function of depth in Moon.

depth	calculated	experimental
180 g/cm^2	2.4 ± 0.2	2.1 ± 0.2
370 g/cm^2	2.6 ± 0.2	2.9 ± 0.3

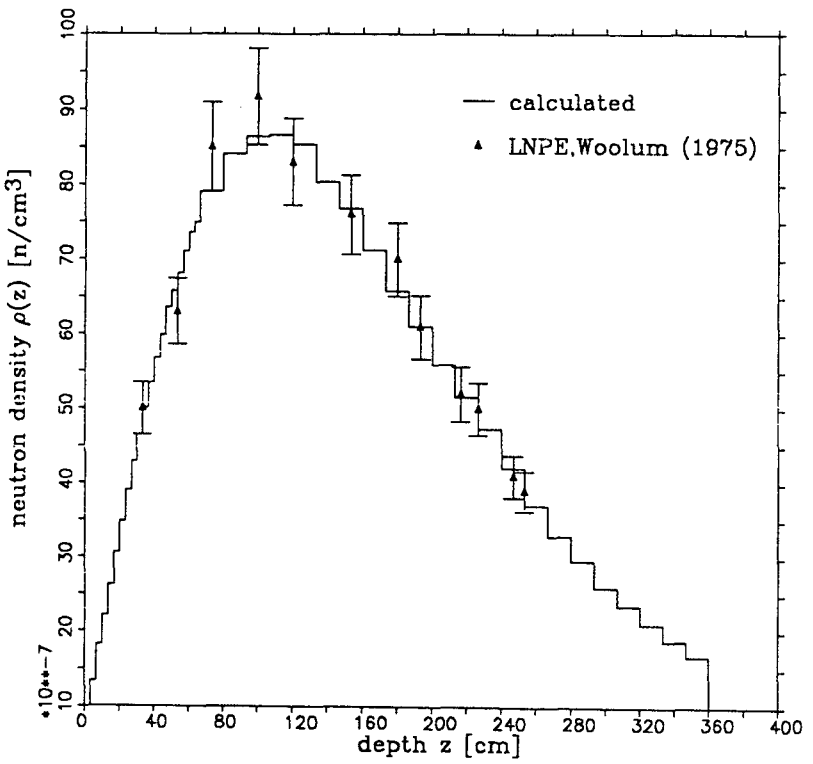

FIG. 1: Calculated neutron density from $^{10}B(n,\alpha)^7Li$ reaction rates as a function of depth in lunar surface compared to experimental results from Ref. (3). $\Phi_{GCR}(4\pi) = 3.0$ p/sec cm^2

Table II: Total gamma albedo for Moon from different mechanisms per incident GCR-particle/sec cm^2 (not including naturally occurring radionuclides)

source	$(n,\gamma),(n,n',\gamma)$	π^0-decay	deexcitation of res. nuclei
$\Phi_\gamma[1/\text{sec cm}^2]$	0.77	1.56	1.13

Total γ-albedo fluxes were obtained together with the neutron fluxes (Tab. II) as a preliminary result. Implementation of gamma ray lines in the coupled n-γ transport calculations is in process.

References:

(1) P. Cloth et al., HERMES User's Guide, Jül-2203, May 1988

(2) D. S. Burnett and D. S. Woolum (1974) Proc. of the 5th Lunar Conf. (Supplement 5,Geochimica et Cosmochimica Acta) Vol. 2,p.2061-2074.

(3) D. S. Woolum et al. (1975) The Moon **12**,p.321-250.

5. Proton Induced Production of Residual Nuclei in the Energy Range from 200 MeV to 5 GeV

P. Dragovitsch

For a considerable number of nuclear reactions only a few and often insufficient production cross section data are available at incident energies above 200 MeV. Systematic measurements of thin target cross sections (e.g. ref./1/) will improve this situation. But large ranges of energies are not covered by accelerators. Here theoretical models can support the experimentel research. Using the INCE-model of HETC/KFA-2 of HERMES code system /2/ calculations of residual nuclei production are done in the energy range between 200 MeV and 5 GeV, delivering mass distributions (Fig.1) or excitation functions (Fig.2).

Most of the calculational approaches to describe the production of residual nuclei by high energy spallation /2-4/ are working successful if small mass differences between target and product are considered. In general at incident energies above some 100 MeV Monte Carlo codes containing a model of the intranuclear cascade followed by an evaporation model deliver the best results. The basic assumption of these models is to treat the nucleus as a Fermi-distributed gas of quasi free nucleons. The intranuclear cascade is performed by single nucleon-nucleon collisions using free particle-particle cross sections. After deexcitation down to some 10 MeV an emission of further particles (up to A = 4) is allowed by evaporation.

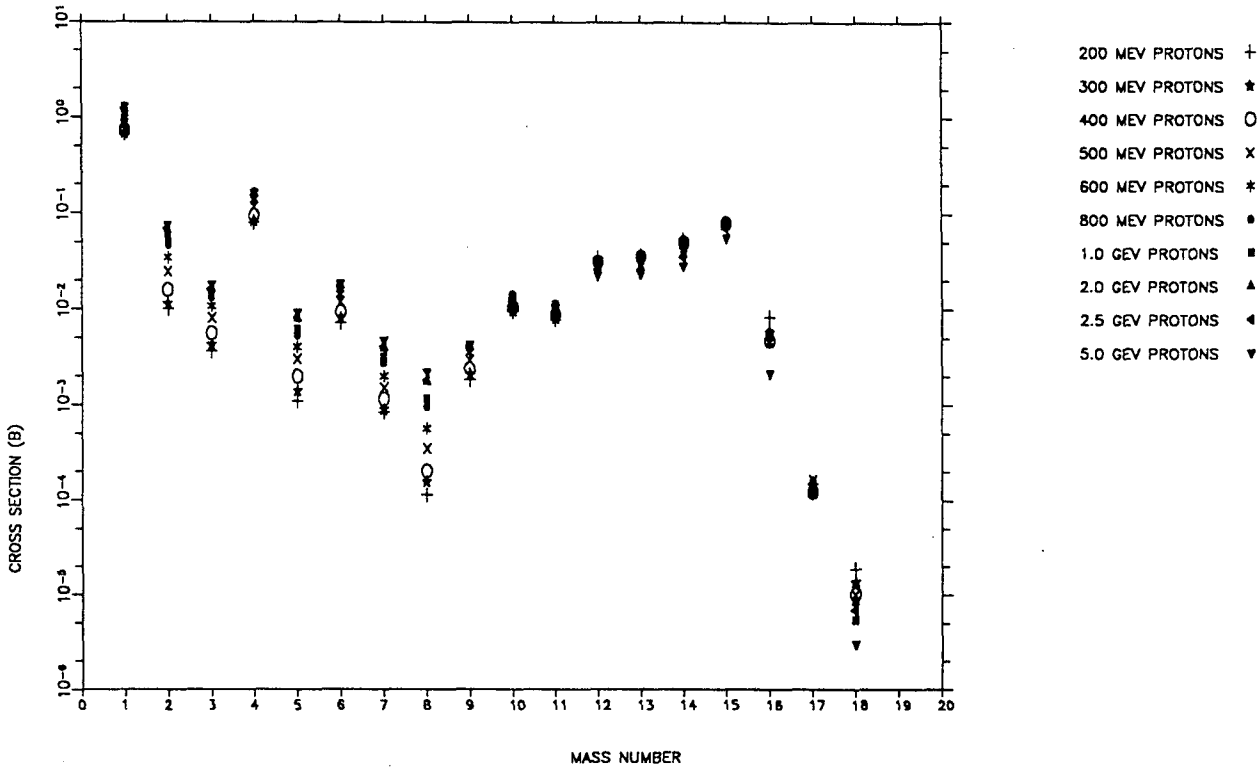

Fig.1: Calculated mass distribution for p-induced spallation products from oxygen

At larger mass differences between target nucleus and observed product even the INCE models fail by a drastic underestimation of the cross sections (Fig.1). In the case of the $O(p,X)^7Be$-reaction the observed differences between the free nucleon model and the experimental data can be interpreted to be a reaction channel containing a complete ^7Be as an ejectile. This indicates that one has to consider a structure of the target nucleus even at excitation energies of several 100 MeV. Detailed measurements of ^7Be in a large region of target masses and various energies were done in the recent years /1,5,6/. The data show a systematically decrease of the cross sections with increasing target masses in the A < 28 region and a continuation with a quasi constant excitation function up

to target masses where single nucleon emission cannot explain the production of this nuclide. Furthermore, at recent measurements of double differential cross sections for charged particle emission ejectile masses of A = 7 have been observed in a not negligible quantity /7/. From these facts one can conclude that even at high excitation energies a emission of light heavy ions with A > 4 has to be considered. Therefore the existance of pretended cluster structures inside the nucleus could be a meaningful explanation. In this context the INCE model is a useful instrument for the selection of possible candidates of nuclear structures because it permits the separation of a reaction into the parts of quasi free interactions and the part attributed to cluster interactions.

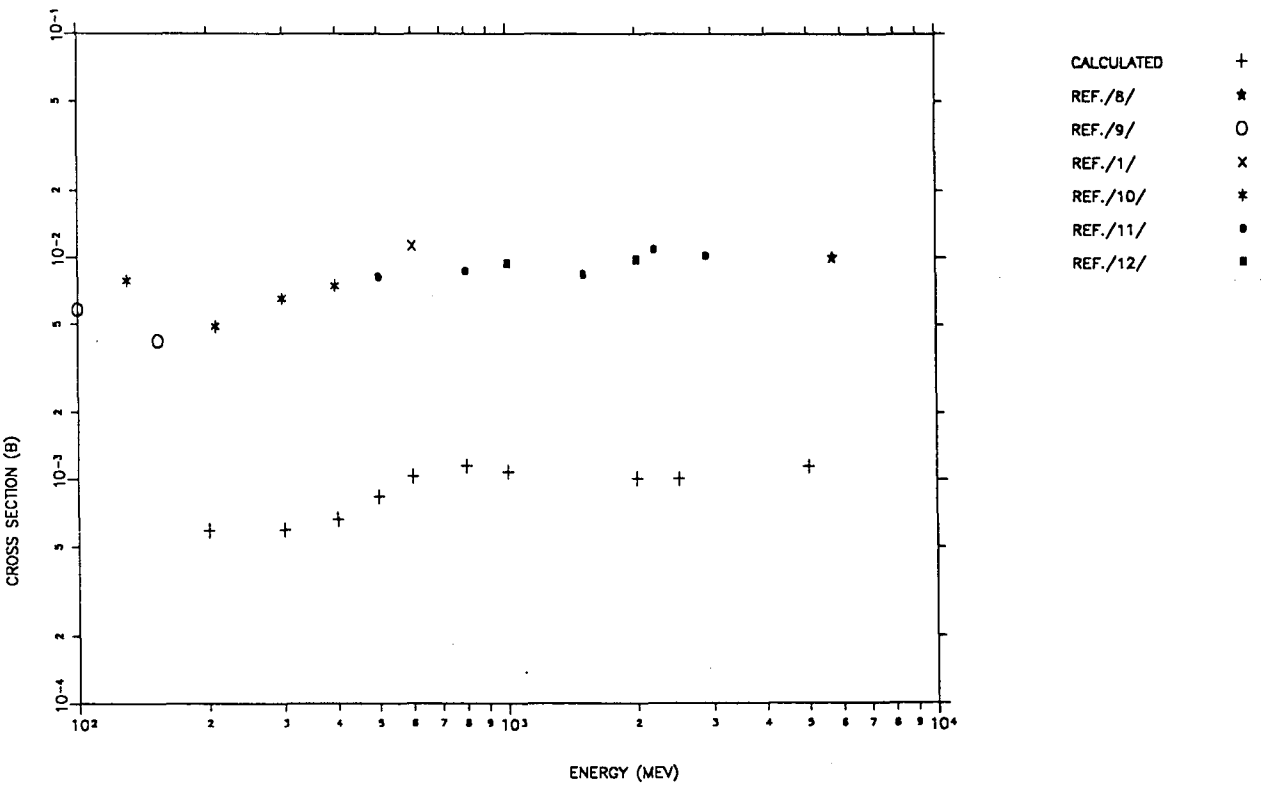

Fig.2: Production cross sections of ^{7}Be from Oxygen: Comparision of INCE-calculations with experimental data.

References:

/1/ P.Dragovitsch et al., (1988), NEANDC(E)-282 U Vol.V, 29-35.
/2/ P.Cloth et al. (1988) Jül-2203
/3/ M.Blann and J.Bisplinghoff (1982) UCID-19614
/4/ J.T.Routti and J.V.Sandberg (1981) Comp. Phys. Com. 23, 411.
/5/ P.Dragovitsch, Thesis, Universität zu Köln
/6/ B.Dittrich et al., (1989), "Proton Induced Spallation Between 600 and 2600 MeV", and references therein, NEANDC(E) (this report).
/7/ K.M.Koch, Thesis, RWTH Aachen, in print
/8/ Benioff (1960) Phys. Rev. 119, 316-324.
/9/ Bimbot and Gauvin (1971) Compt. Rend. Ser. B273, 1054-1057.
/10/ G.V.S.Rayudu (1964) Nucl. Chem. Res. Ann. Rep. 1963-1964, 7.45
/11/ G.V.S.Rayudu (1968) J. Inorg. Nucl. Chem. 30, 2311.
/12/ G.M.Raisbeck and F.Yiou (1975) Phys. Rev. C12, 915-920.

GKSS-FORSCHUNGSZENTRUM GEESTHACHT GMBH
INSTITUT FÜR PHYSIK

14 MeV Neutron Activation Cross-Sections

H.M. Agrawal, R. Pepelnik, Y. Tian, E. Bössow

Accurate 14 MeV neutron activation cross-sections are needed for dosimetry, for calculating the activation of materials to be used in future fusion reactors and for routine multielemental 14 MeV neutron activation analysis of various kinds of samples at neutron generator facilities such as KORONA [1]. Several uncertain cross-sections of Cu, Y, Ag, Sb, La and Yb have been remeasured.

Samples of Cu and Ag pure metallic foils and of Y, Y_2O_3, Ag_2O_3, Sb_2O_3, La_2O_3 and Yb in powdered form were investigated in the present work. The purity of the material was better than 99 %.

Employing the well-known excitation function of the reactions ^{90}Zr(n,2n) [2] and ^{93}Nb(n,2n) [3] the neutron energy at the centre of the cylindrical target of KORONA was determined to a median at 14.6 MeV and a FWHM of 0.6 MeV. For the neutron flux monitoring a long-counter is used. The long-counter has been calibrated via the well-known cross-section of the reaction ^{27}Al(n,α) [4].

The reaction cross-sections determined are summarized in Table I and Table II.

Table I Activation Cross-Sections (mbarn) at 14.6 ± 0.3 MeV

Reaction	Half Life	Isotop. Abund. (%)	This Work 14.6±0.3 MeV	Literature Values between 14.4. and 14.8 MeV (mbarn)	(mbarn)
^{65}Cu(n,p)^{65}Ni	2.52 h	30.83	22±1	20±1 [5]	20.5±1.4 [6]
^{65}Cu(n,α)^{62m}Co	13.9 m	30.83	5.9±0.3	7.9±1.7 [7]	7.2±2.1 [8]
^{89}Y(n,α)^{86m}Rb	61.0 s	100.	1.78±0.06	0.91±0.45 [9]	1.0±0.4 [10]
^{89}Y(n,n')^{89m}Y	16.1 s	100.	451±22	438±44 [11]	352±43 [12]
^{89}Y(n,2n)^{88}Y	107 d	100.	950±75	946±14 [13]	907±68 [10]
^{107}Ag(n,n')^{107m}Ag	44.3 s	51.84	294±12	312±77 [14]	304 [7]
^{107}Ag(n,p)^{107m}Pd	21.3 s	51.84	7.5±0.3	10.8 [7]	15±2 [10]
^{109}Ag(n,n')^{109m}Ag	39.6 s	48.16	292±12	419±77 [14]	291 [7]
^{109}Ag(n,p)^{109m}Pd	4.69 m	48.16	4.6±0.8	9.4±1.3 [14]	5.8 [7]
^{121}Sb(n,2n)^{120}Sb	5.76 d	57.3	507±15	427±20 [15]	546±20 [5]
^{139}La(n,p)^{139}Ba	84.6 m	99.91	4.43±0.22	6.0±0.6 [16]	3.7 [7]
^{139}La(n,α)^{136}Cs	13.2 d	99.91	2.57±0.12	2.4±0.2 [17]	2.5±0.3 [16]
^{174}Yb(n,p)^{174}Tm	5.4 m	31.8	3.11±0.14	3.0±0.2 [18]	2.7 [7]
^{174}Yb(n,α)^{171}Er	7.52 h	31.8	1.12±0.11	1.26±0.2 [19]	1.22±0.23[20]
^{176}Yb(n,p)^{176}Tm	1.9 m	12.7	1.44±0.08	1.8 [7]	
^{176}Yb(n,α)^{173}Er	1.4 m	12.7	0.56±0.05	0.7 [7]	
^{176}Yb(n,n'p)^{176m}Yb	11.4 s	12.7	18.5±1.2	19.7±1.7 [18]	16.7±3.5[21]

Table II Elemental and Isotopic Cross-Sections at 14.6 ± 0.3 MeV

Reaction	Half Life	This Work 14.6±0.3 MeV	Isotop. Abund. (%)	Literature Values between 14.4. and 14.8 MeV (mbarn)	(mbarn)
$Sb(n,x)^{122m+g}Sb$	2.70 d	770±23	42.7	1542±80 [15]	1420±140[8]
$Yb(n,x)^{172}Tm$	63.6 h	1.11±0.09	21.9		
$Yb(n,x)^{173}Tm$	8.24 h	0.92±0.06	16.1	13.5 [20]	

The neutron energy spectrum within the cylindrical target of KORONA also contains contributions from elastically and inelastically scattered neutrons. These contributions have been calculated [22, 23] to 26 and 9 % of the total neutron flux, respectively. The scattered neutrons of lower energy might have influenced the effective activation cross-section.

References

[1] H.-U. Fanger, R. Pepelnik, W. Michaelis, J. Radioanal. Chem. 61 (1981) 147.
[2] A. Pavlik, G. Winkler, H. Vonach et al., J. Phys. G 8 (1982) 1283.
[3] T.B. Ryves, private communication, to be published.
[4] G. Winkler, T.B. Ryves, Ann. nucl. Energy Vol.10, No.11 (1983) 601.
[5] B.M. Bahal, E. Bössow, M. Farooq, R. Pepelnik, GKSS 86/E/29 (1986).
[6] B.P. Evain, D.L. Smith, P. Lucchese, ANL/NDM-89 (1985).
[7] V. McLane, Ch.L. Dunford, Ph.F. Rose, Neutron Cross Sections, Vol. 2 (1988) Acad. Press, San Diego.
[8] V.M. Bychkov et al., Cross sections for neutron induced threshold reactions, Energoizdat, Moscow (1982).
[9] E.T. Bramlitt, R.W. Fink, Physical Review 131 (1963) 2649.
[10] S.M. Qaim, 14 MeV neutron activation cross sections, Handbook of Spectroscopy, Vol. III (1981) 141, CRC Press, Boca Rota.
[11] Z. Bödy, J. Csikai in Handbook on Activation Data, Techn. Report Ser. No. 273, IAEA 1987, p. 285.
[12] A. Abboud et al., Acta Phys. Polonica B2 (1971) 527.
[13] M. Wagner et al., IRK Progr. Rep. 1987/1988, Vienna.
[14] W. Augustyniak, M. Herman, A. Marcinkowski, Nucl. Physics A 247 (1975) 231.
[15] Wen-Deh Lu, N. RanaKumar, R.W. Fink, Physical Review C1 (1970) 350.
[16] A. Bari, J. Radioanalytical Chemistry 75 (1982) 189.
[17] R. Wölfle et al., Appl. Radiat. Isotop., Vol. 39 (1988) 407.
[18] B. Anders, R. Pepelnik, H.-U. Fanger in K.H. Böckhoff (ed.), Nuclear Data for Science and Technology (1982) 859, Antwerp.
[19] S.M. Qaim, Radiochimica Acta 35 (1984) 5.
[20] T. Sato et al., J. Nucl. Science and Techn. (Japan) 12/11 (1975) 681.
[21] P. Bornemisza-Pauspertl et al., B. österr. Akad. d. Wiss. 176 (1968) 227.
[22] B.M. Bahal, H.-U. Fanger, Nucl. Instr. and Meth. 211 (1983) 469.
[23] A. Pavlik, G. Winkler, Inst. für Radiumforschung und Kernphysik der Universität Wien, to be published.

ABTEILUNG NUKLEARCHEMIE
UNIVERSITÄT ZU KÖLN

ZENTRALEINRICHTUNG FÜR STRAHLENSCHUTZ
UNIVERSITÄT HANNOVER

1. Proton-Induced Spallation between 600 and 2600 MeV

B. Dittrich[1], U. Herpers[1], M. Lüpke[2], R. Michel[2]

1.1 Production of Residual Nuclides by Proton-Induced Spallation between 600 MeV and 2600 MeV.

In the course of a research programm to investigate the transition from preequilibrium to spallation reactions, done in collaboration of groups from Cologne, Hannover, Jülich and Zürich, thin-target cross sections for the production of stable and radioactive nuclides by proton-induced reactions on O, Mg, Al, Si, Ca, Ti, V, Mn, Fe, Co, Ni, Cu, Zr, Rh, Ba, and Au were determined at 800, 1200 and 2600 MeV using accelerators at LANL/Los Alamos and at LNS/Saclay. Gamma- and X-spectrometry as well as conventional and accelerator mass spectrometry are used to measure the residual nuclides. Table 1 gives a survey on the target/product-combinations under investigations. Final results were obtained for short- and medium-lived nuclides for target elements from O to Rh. The measurements for Ba and Au and for some selected long-lived nuclides from other target elements as well as the data evaluation still are going on. Also the mass spectrometric measurements are not yet finished. Exemplarily, in table 2 cross sections for the production of radionuclides from natural iron are presented. The target element Fe, which has been investigated quite often in the past, is an excellent example to demonstrate the need for high accuracy cross sections if one wants to improve the understanding of high energy nuclear reactions. Many of the experimental data reported in the past suffer from severe problems, so that there is an uncertainty of up to one order of magnitude when looking for non-evaluated experimental data, see e.g. data for the reaction Fe(p,2pxn)^{52}Mn in fig. 1.

1 Nuklearchemie Köln, 2 Zentraleinr. für Strahlenschutz Hannover

Table 1: Survey on target/product-combinations investigated by irradiation experiments at LANL/Los Alamos and LNS/Saclay in the energy range 800 MeV $\leq E_p \leq$ 2600 MeV.

Target	Product Nuclides Measured By								
	Gamma- and X-spectrometry				AMS			MS	
Oxygen	^{7}Be				^{10}Be	^{14}C		He	
Magnesium	^{7}Be	^{22}Na	^{24}Na		^{10}Be	^{14}C	^{26}Al	He	Ne
Aluminum	^{7}Be	^{22}Na	^{24}Na		^{10}Be	^{14}C	^{26}Al	He	Ne
Silicon	^{7}Be	^{22}Na	^{24}Na	^{28}Mg	^{10}Be	^{14}C	^{26}Al	He	Ne
Calcium	^{7}Be ^{42}K ^{46}Sc	^{22}Na ^{43}K ^{47}Sc	^{24}Na ^{47}Ca ^{48}Sc	^{28}Mg ^{44m}Sc	^{10}Be	^{26}Al			
Titanium	^{7}Be ^{42}K ^{46}Sc ^{48}V	^{22}Na ^{43}K ^{47}Sc	^{24}Na ^{47}Ca ^{48}Sc	^{28}Mg ^{44m}Sc ^{44}Ti	^{10}Be	^{26}Al	^{41}Ca	He Ar	Ne
Vanadium	^{7}Be ^{42}K ^{46}Sc ^{48}V	^{22}Na ^{43}K ^{47}Sc ^{51}Cr	^{24}Na ^{47}Ca ^{48}Sc	^{28}Mg ^{44m}Sc ^{44}Ti	^{10}Be	^{26}Al			
Manganese	^{7}Be ^{42}K ^{46}Sc ^{48}V	^{22}Na ^{43}K ^{47}Sc ^{51}Cr	^{24}Na ^{47}Ca ^{48}Sc ^{52}Mn	^{28}Mg ^{44m}Sc ^{44}Ti ^{54}Mn	^{10}Be	^{26}Al			
Iron	^{7}Be ^{42}K ^{47}Sc ^{51}Cr ^{57}Co	^{22}Na ^{43}K ^{48}Sc ^{52}Mn ^{58}Co	^{24}Na ^{44m}Sc ^{44}Ti ^{54}Mn	^{28}Mg ^{46}Sc ^{48}V ^{56}Co	^{10}Be ^{41}Ca	^{14}C	^{26}Al	He Ar	Ne
Cobalt	^{7}Be ^{42}K ^{47}Sc ^{52}Mn ^{57}Co	^{22}Na ^{43}K ^{48}Sc ^{54}Mn ^{58}Co	^{24}Na ^{44m}Sc ^{48}V ^{55}Co ^{56}Ni	^{28}Mg ^{46}Sc ^{51}Cr ^{56}Co ^{57}Ni	^{10}Be	^{26}Al			
Nickel	^{7}Be ^{42}K ^{48}V ^{55}Co ^{60}Co	^{22}Na ^{43}K ^{51}Cr ^{56}Co ^{56}Ni	^{24}Na ^{44m}Sc ^{52}Mn ^{57}Co ^{57}Ni	^{28}Mg ^{46}Sc ^{54}Mn ^{58}Co	^{10}Be ^{41}Ca	^{14}C	^{26}Al	He Ar	Ne

Table 1: (continued) Survey on target/product-combinations investigated by irradiation experiments at LANL/Los Alamos and LNS/Saclay in the energy range 800 MeV $\leq E_p \leq$ 2600 MeV.

Target	Product Nuclides Measured By Gamma- and X-spectrometry								MS
Copper	^{7}Be	^{22}Na	^{24}Na	^{28}Mg	^{42}K	^{43}K	^{44m}Sc	^{46}Sc	
	^{48}V	^{51}Cr	^{52}Mn	^{54}Mn	^{55}Co	^{56}Co	^{57}Co	^{58}Co	
	^{60}Co	^{56}Ni	^{57}Ni	^{65}Zn					
Zirconium	^{7}Be	^{22}Na	^{46}Sc	^{48}V	^{51}Cr	^{52}Mn	^{54}Mn	^{59}Fe	Kr
	^{56}Co	^{58}Co	^{60}Co	^{65}Zn	^{67}Ga	^{69}Ge	^{74}As	^{75}Se	
	^{76}Br	^{79}Kr	^{83}Rb	^{84}Rb	^{83}Sr	^{87}Y	^{88}Y	^{91}Y	
	^{88}Zr	^{89}Zr	^{95}Zr	^{90}Nb					
Niobium	^{7}Be	^{46}Sc	^{48}V	^{51}Cr	^{54}Mn	^{59}Fe	^{56}Co	^{58}Co	Kr
	^{60}Co	^{65}Zn	^{67}Ga	^{69}Ge	^{74}As	^{75}Se	^{79}Kr	^{83}Rb	
	^{84}Rb	^{83}Sr	^{87}Y	^{91}Y	^{88}Zr	^{89}Zr	^{90}Nb	^{92m}Nb	
Rhodium	^{48}V	^{58}Co	^{65}Zn	^{71}As	^{74}As	^{75}Se	^{79}Kr	^{84}Rb	
	^{87}Y	^{91}Y	^{86}Zr	^{88}Zr	^{89}Zr	^{90}Nb	^{92m}Nb	^{95}Nb	
	^{97}Ru	^{99}Rh	^{100}Rh	^{101m}Rh	^{101}Rh	^{102}Rh	^{102m}Rh		
Barium	^{127}Xe	^{134}Cs	^{136}Cs	^{131}Ba	^{133}Ba				Xe
Gold	^{185}Os	^{188}Ir	^{189}Ir	^{190}Ir	^{192}Ir	^{188}Pt	^{191}Pt	^{194}Au	
	^{195}Au	^{196}Au							

The observed uncertainty in non-evaluated experimental data does not allow for stringent tests of nuclear reaction models, nor is it tolerable for the various applications of high energy integral cross sections as e.g. in astro- and cosmophysics. The new data, however, together with those reported earlier for a proton energy of 600 MeV [1-3] represent a consistent data set of thin-target cross sections of more than 300 individual spallation reactions. Together with the data for proton energies up to 200 MeV measured earlier by our group [4,5, and references therein] they give the complete excitation functions from the thresholds up to 2600 MeV. Fig. 1 displays this for the reaction Fe(p,2pxn)^{52}Mn. Further irradiation experiments at 350 MeV and between 50 and 200 MeV are in preparation in order to complete the now existing data base by closing the energy gap between 200 and 600 MeV and by investigating those target elements in the low-energy region which were not dealt with earlier.

Table 2: Cross sections [mb] for the production of radionuclides from natural iron.

Reaction	Cross Section [mb] at 800 MeV	1200 MeV	2600 MeV
FE(P,23pXn)^{7}Be	3.12 +- 0.23	5.26 +- 0.40	8.33 +- 0.61
Fe(p,16pXn)^{22}Na	0.780 +- 0.061	1.62 +- 0.12	2.52 +- 0.20
Fe(p,16pXn)^{24}Na		2.04 +- 0.15	3.57 +- 0.26
Fe(p,8pXn)^{42}K		4.02 +- 0.32	3.61 +- 0.31
Fe(p,8pXn)^{43}K	1.35 +- 0.19	1.35 +- 0.10	1.18 +- 0.09
Fe(p,6pXn)^{44m}Sc	8.73 +- 0.62	7.96 +- 0.57	6.36 +- 0.45
Fe(p,6pXn)^{46}Sc	10.0 +- 0.7	9.47 +- 0.71	7.12 +- 0.51
Fe(p,6pXn)^{48}Sc		0.590 +- 0.046	0.511 +- 0.040
Fe(p,4pXn)^{48}V	21.9 +- 1.6	19.4 +- 1.4	14.8 +- 1.1
Fe(p,3pXn)^{48}Cr		0.803 +- 0.062	0.639 +- 0.051
Fe(p,3pXn)^{51}Cr	44.4 +- 3.2	41.3 +- 3.1	33.4 +- 2.4
Fe(p,2pXn)^{52}Mn	10.5 +- 0.7	9.29 +- 0.66	8.64 +- 0.62
Fe(p,2pXn)^{54}Mn	42.6 +- 3.0	42.6 +- 3.2	36.8 +- 2.6
Fe(p,Xn)^{56}Co	1.63 +- 0.12	1.80 +- 0.13	1.71 +- 0.13
Fe(p,Xn)^{57}Co	0.355 +- 0.026	0.453 +- 0.032	0.518 +- 0.039
Fe(p,Xn)^{58}Co	0.0652 +- 0.0091	0.071 +- 0.013	0.121 +- 0.014

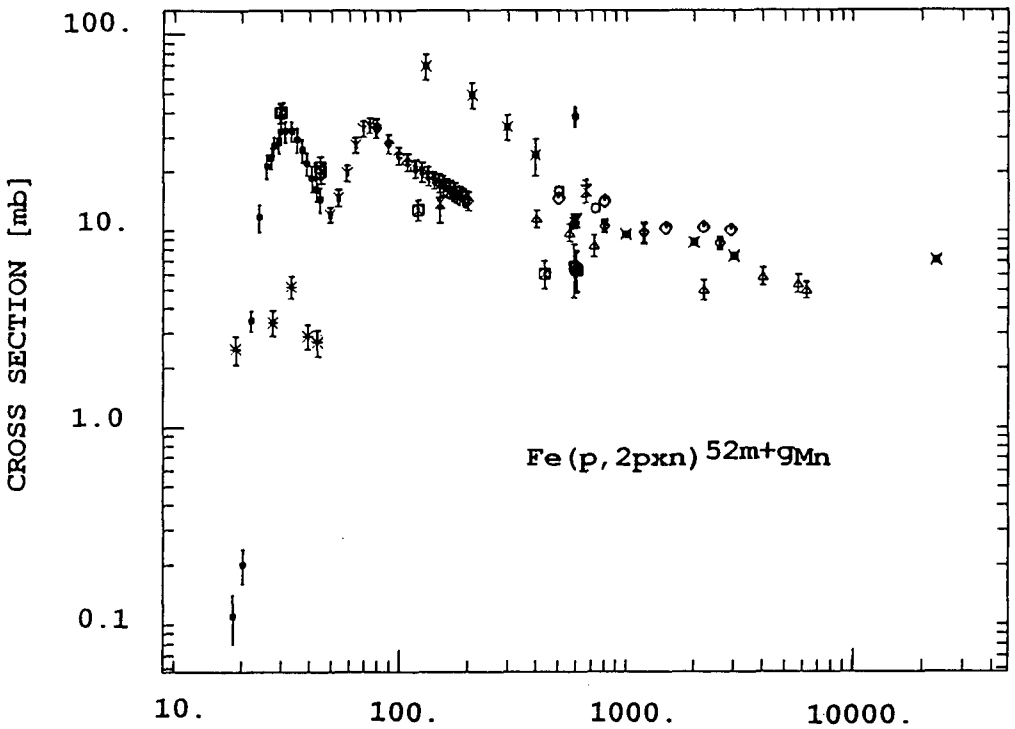

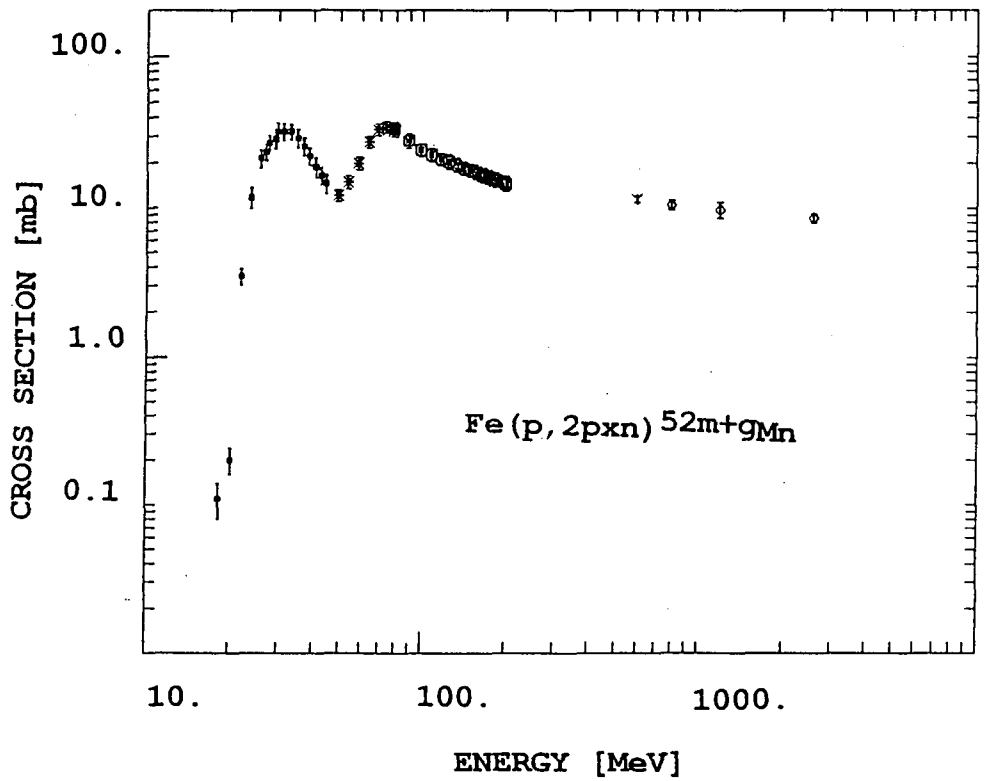

Fig. 1: Comparison of all experimental cross sections available up to now (upper part) for the reaction Fe(p,2pxn)^{52}Mn with the excitation function measured by our group (lower part).

1.2 Calculation of Production Cross Sections by Semiempirical Models and by Monte Carlo Modelling of the Intranuclear Cascade.

Though not all experimental cross sections are available right now, it is possible to do some comparison of the new data with the results of model calculations. The existing data already now allow a discussion of the quality of parametric models [6,7], which are often used for the calculation of spallation cross sections. In figs. 2 and 3 the results of a comparison of our new experimental data with those calculated by Rudstam's CDMDG formula [6] and by the formula proposed by Silberberg and Tsao [7] are given for all three proton energies. The calculations were done by the code SPALL by Routti and Sandberg [8]. A comparison of theoretical and experimental data shows partially severe discrepancies. Though considerable improvements have been achieved in the more recent formula [7], in particular with respect to the production of light fragments, for many nuclides theory and experiment deviate by more than a factor of two. It has to be emphasized that the calculational accuracy obtained so far is not sufficient for the application of these formulas in astro- and cosmophysics. On the other hand, one has to consider that the parameterizations on which the semi-empirical formulas are based were performed with the strongly insufficient data base existing at that time. It may be worthwile to look for the quality obtainable by these parametric models when applying the new experimental data for a re-parameterization.

Another, more physical approach to describe high-energy nuclear reactions is to model the intranuclear cascade by Monte Carlo calculations and to derive absolute production cross sections by evaluating the history of residual nuclei. Such calculations were performed using the high energy transport code HETC/KFA-2 within the newly developed HERMES code system [9]. A detailed description of the calculational method has been given elsewhere [1]. As can be seen from figs. 4 - 7 the results are rather encouraging. For energies above 600 MeV the calculated excitation functions nicely match the experimental ones. The agreement is excellent for the production of ^{22}Na, ^{48}V and ^{56}Co from Fe, while some deviations are seen for that of ^{54}Mn. Presently, these calculations are extended to other target elements, in particular to monoisotopic ones, for which there is no ambiguity regarding the contributing reaction channels. On the basis of the new experimental data it will be possible to obtain a systematic survey on the capabilities of the model used and thus to come to a better understanding of high energy nuclear reactions in general.

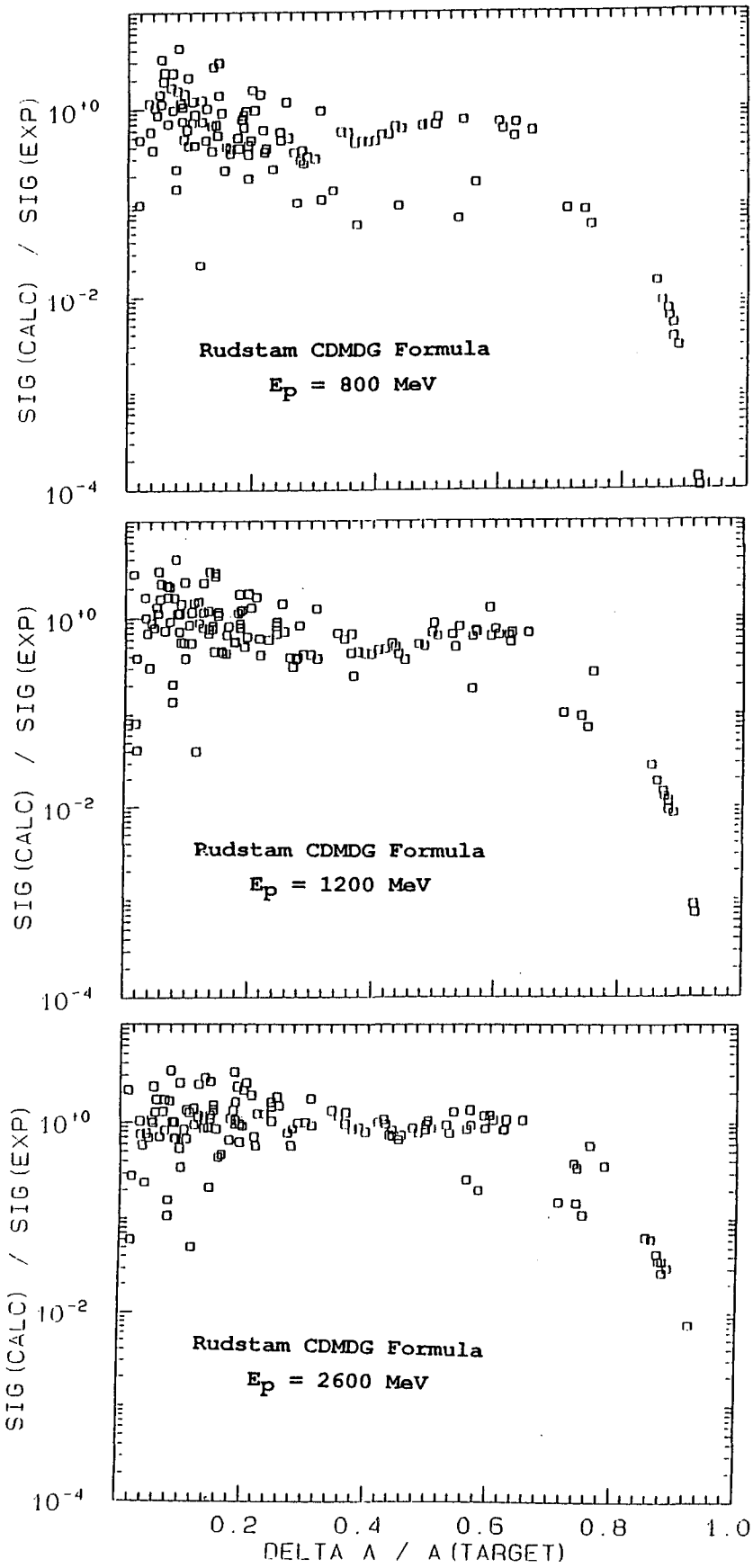

Fig. 2: Ratios of cross sections calculated by the semiempirical CDMDG formula of Rudstam [6] and of experimental ones from this work for proton energies of 800, 1200 and 2600 MeV.

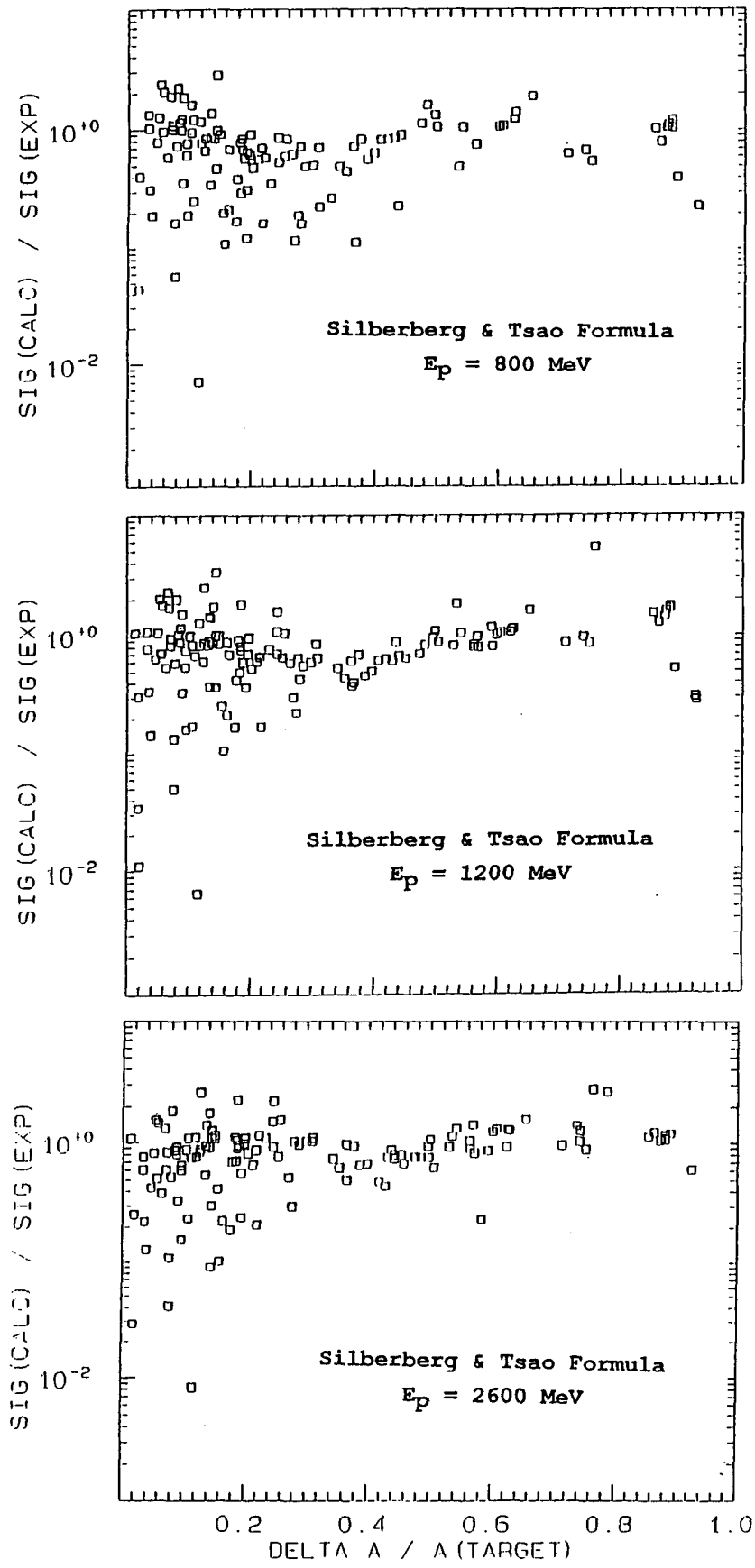

Fig. 3: Ratios of cross sections calculated by the semiempirical formula of Silberberg and Tsao [7] and of experimental ones from this work for proton energies of 800, 1200 and 2600 MeV.

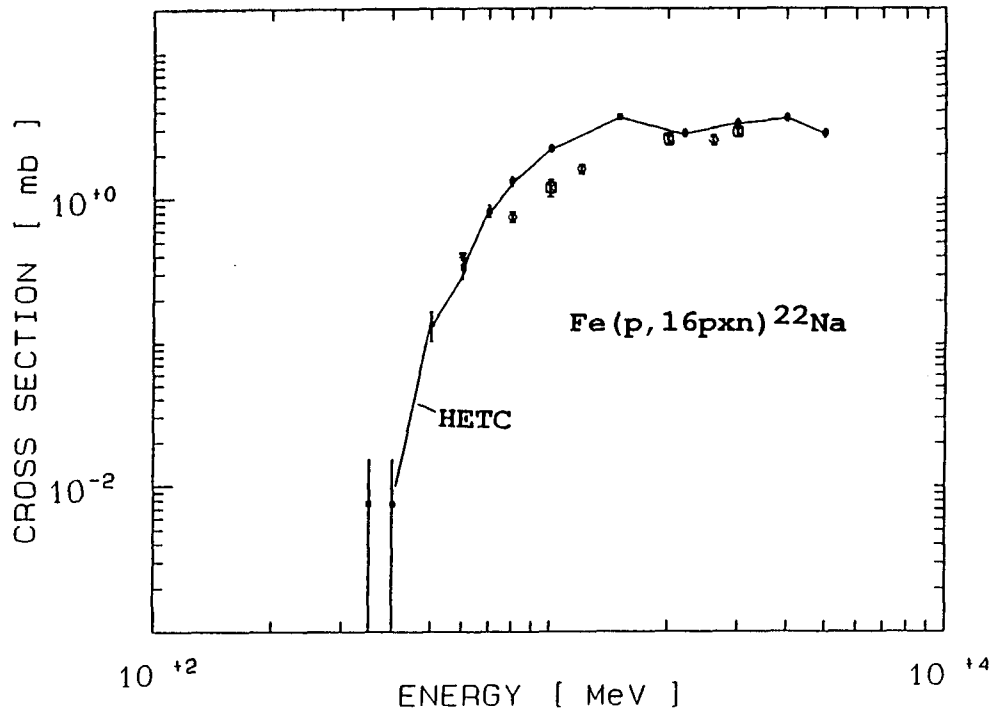

Fig. 4: Experimental excitation function for the production of ^{22}Na from natural iron compared with HETC calculations. The experimental cross sections are restricted to data measured by our group and by Raisbeck and Yiou [10].

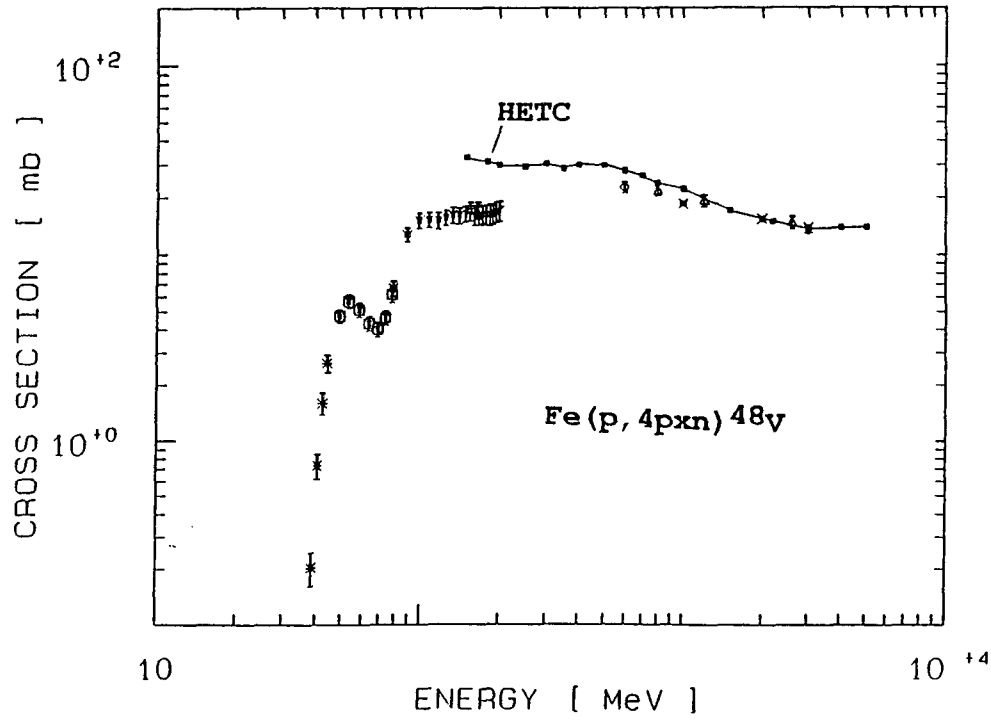

Fig. 5: Experimental excitation function for the production of ^{48}V from natural iron compared with HETC calculations. The experimental cross sections are restricted to data measured by our group and by Raisbeck and Yiou [10].

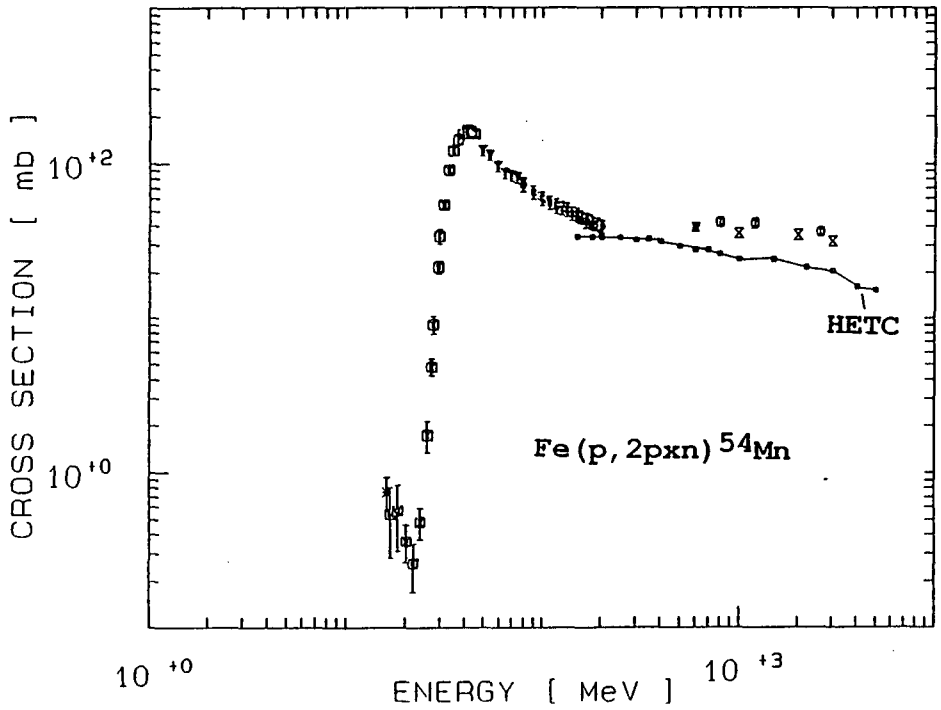

Fig. 6: Experimental excitation function for the production of ^{54}Mn from natural iron compared with HETC calculations. The experimental cross sections are restricted to data measured by our group and by Raisbeck and Yiou [10].

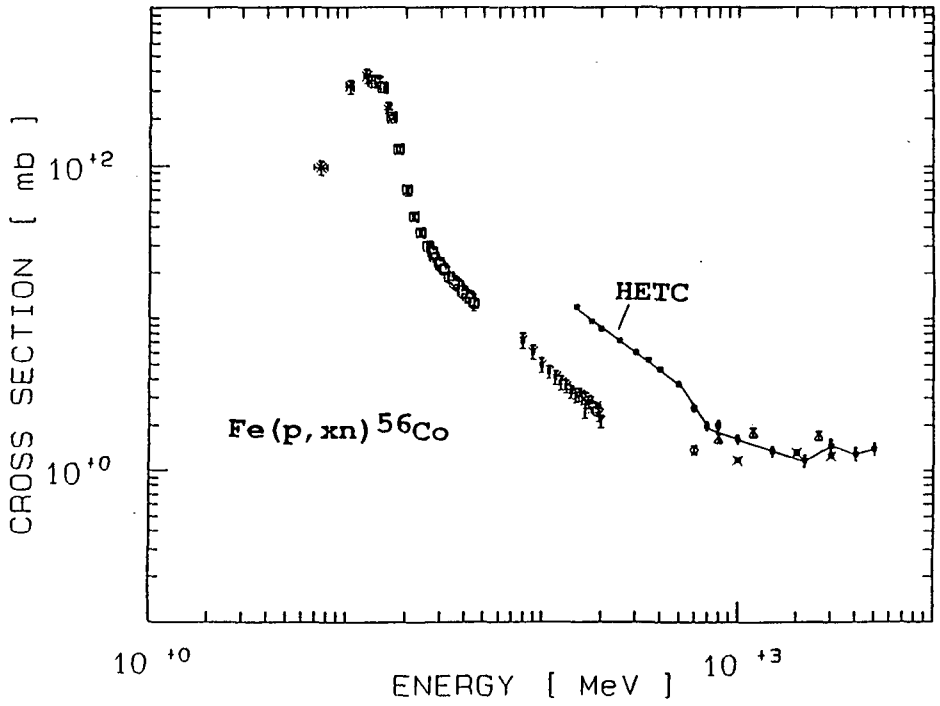

Fig. 7: Experimental excitation function for the production of ^{56}Co from natural iron compared with HETC calculations. The experimental cross sections are restricted to data measured by our group and by Raisbeck and Yiou [10].

References

[1] R. Michel, B. Dittrich, U. Herpers, T.Schiffmann, P. Cloth, P. Dragovitsch, D. Filges, Proton-induced spallation at 600 MeV, Proc. 2nd Int. Conf. on Nuclear and Radiochemistry, July 11th-15th 1988, Brighton, The Analyst, in press, 1989

[2] R. Michel, F. Peiffer, S. Theis, F. Begemann, H. Weber, P. Signer, R. Wieler, P. Cloth, P. Dragovitsch, D. Filges, P. Englert, Production of stable and radioactive nuclides in thick stony targets (R = 15 and 25 cm) isotropically irradiated with 600 MeV protons - Simulation of production of cosmogenic nuclides in meteorites, Nucl. Instr. Meth. Phys. Res. B, in press, 1989.

[3] R. Michel, P. Dragovitsch, K. Prescher, M.N. Rao, J. Methew, in: Progress Report on Nuclear Data Research in the Federal Republic of Germany for the Period April, 1st, 1987 to March, 31th, 1988, NEANDC(E)-292 U Vol. V INDC(Ger)-32/LN+Special, 1988, 25.

[4] R. Michel, R. Stück, J. Geophys. Res. (Suppl.) 89 B (1984) 673.

[5] R. Michel, F. Peiffer, R. Stueck, Nucl. Phys. A 441 (1985) 617.

[6] G. Rudstam, Z. Naturf. 21a (1966) 1027.

[7] R. Silberberg, C.H. Tsao, Astrophys. J. Suppl. 25 (1973) 315.

[8] J.T. Routti, J.V. Sandberg, Comp. Phys. Comm. 23 (1981) 411.

[9] P. Cloth, D. Filges, R.D. Neef, G. Sterzenbach, C. Reul, T.W. Armstrong, B.L. Colburn, Jül-2203 (1988).

[10] G.M. Raisbeck, F. Yiou, Phys. Rev. C 9 (1975) 915.

This work was supported by the Deutsche Forschungsgemeinschaft.

INSTITUT FÜR KERNCHEMIE
UNIVERSITÄT MAINZ

Isomeric Ratios and Independent Yields of ^{134}I and ^{136}I in the Reactor Neutron Induced Fission of ^{232}Th.

R. Hentzschel and H. O. Denschlag

The isomeric formation ratios and the fractional independent yields of ^{134}I and ^{136}I have been measured in the reactor neutron induced fission of ^{232}Th using a fast radiochemical separation of iodine from the rest of the fission products. The separation is based on the ion exchange of iodide with a preformed precipitate of silver chloride and takes a time of 2 sec. The chemical yield of the exchange amounts to 90 %. The decontamination factors obtained with respect to the other fission products are generally 1200.

The irradiations were carried out in the Mainz TRIGA reactor using the pulse mode that provides neutron bursts of 100 ms duration and a fast neutron fluence of about 1-2·10^{12} n/cm^2 (neutron energy ≥ 0.4 eV). The samples (0.5 g thorium as nitrate in 1.5 ml 2 M HNO_3 sealed in polystyrene capsules) were shot into a separation unit (Fig. 1) directly after the pulse using a pneumatic system. The capsules broke in the separation unit by the impact and the fission product solution

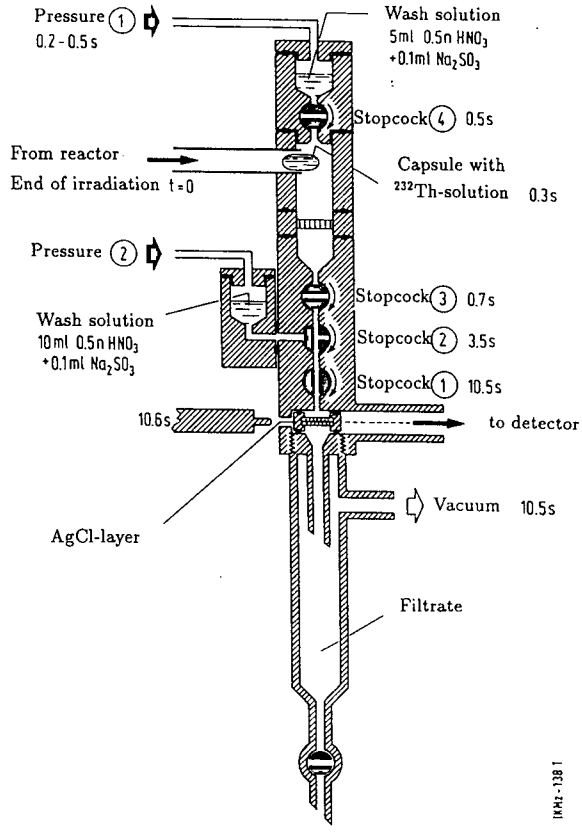

Fig.1: Automatic separation unit and time sequence.

was filtered through the AgCl layer immediately or after known waiting times. A wash solution was passed through the AgCl layer and the filter unit was shot pneumatically into a shielded counting position. The gamma-ray spectra were measured at short intervals for the growth and decay curve analysis of the iodine isotopes and their daughter products. The waiting times between arrival of the samples and the filtration through the AgCl layer were used to observe the growth of the iodine isotopes from their tellurium precursors and, hence to determine their fractional independent yields.

The following values were obtained for the fractional independent yields (Y_{FI}) and the fractions of high spin isomer ($F_H = Y_H/(Y_L+Y_H)$):

^{134}I: $Y_{FI} = 1.6\ \% \pm 0.4\ \%$ $F_H = 0.47 \pm 0.05$

^{133}I: $Y_{FI} = 33.7\ \% \pm 6\ \%$ $F_H = 0.71 \pm 0.05$

These values together with the other fractional yields known for this fission process [1] were submitted to an analysis within the framework of Wahl's Z_p-model [2]. This analysis confirmed the strong odd-even pairing effect for protons of about 28 % and, hence the low excitation energy of thorium fission.

The isomeric ratios were used to derive the root mean square angular momenta (J_{rms}) of the corresponding fission fragments at scission using the simple statistical model of Madland and England [3]. The values obtained are listed in the following:

^{134}I: $J_{rms} = 8.0 \pm 0.7\ \hbar$

^{136}I: $J_{rms} = 8.5 \pm 1.0\ \hbar$

These measurements are the first results on angular momenta in the fission of thorium. They show that low excitation energies at scission are well compatible with high angular momenta of the fission fragments. The present work is described in detail in Ref. [4].

References

[1] A. Srivastava, and H. O. Denschlag, Radiochim. Acta 46, 17 (1989)

[2] A.C. Wahl, Atomic Data and Nuclear Data Tables, 39, 1 (1988)

[3] D. G. Madland, R. England, Nuclear Science and Engineering, 64, 859 (1977)

[4] R. Hentzschel, Diplomarbeit, Mainz (1989) in German, to be published.

FRM-REAKTORSTATION GARCHING, FACHBEREICH PHYSIK
TECHNISCHE UNIVERSITÄT MÜNCHEN

1. Scattering of Slow Neutrons by Thorium

W. Waschkowski, K. Knopf, L. Koester

In continuation of our previous studies on slow neutron scattering we determined by means of the Christiansen filter technique and transmission measurements the following quantities for thorium:

- the coherent scattering length	$b = 10.31 \pm 0.03$ fm,
- the absorption cross section at 0.0253 eV	$\sigma_\gamma = 7.34 \pm 0.09$ b,
- the potential radius	$R' = 9.6 \pm 0.2$ fm.

In combination with scattering cross sections in the eV-energy region we obtained information about bound levels at negative energies.

Published in Z. Naturforschung 44 (1989) 173

INSTITUT FÜR KERNENERGETIK UND ENERGIESYSTEME
UNIVERSITÄT STUTTGART

1. Validation and Benchmark Testing of Evaluated Neutron Cross Sections for Hydrogen and Deuterium in the Liquid Phase [1]

W. Bernnat, D. Emendörfer, J. Keinert, M. Mattes

Continuing our studies of the neutron scattering dynamics in cold moderators [1] we have derived for liquid hydrogen and deuterium improved differential and integral neutron cross sections taking into account intramolecular as well as intermolecular interactions. For the total scattering cross sections the consideration of intermolecular interference is more (Fig. 2) or less (Fig. 1) important. The good agreement between theory and experiment is obtained by synthetic structure factors $S(\kappa)$ for H_2 and D_2 [1]. For comparison cross sections calculated with the Young-Koppel-model [2] and with the gas model are also shown.

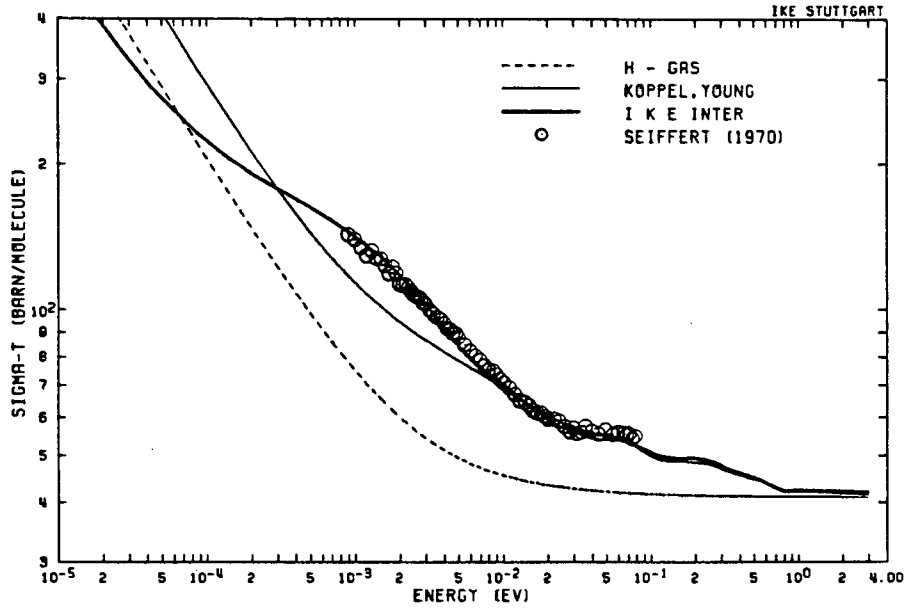

Fig. 1: Total neutron cross sections for normal-hydrogen (n-H_2) at T = 16 K

[1]funded by BMFT, Project 'Erforschung kondensierter Materie und Atomphysik'

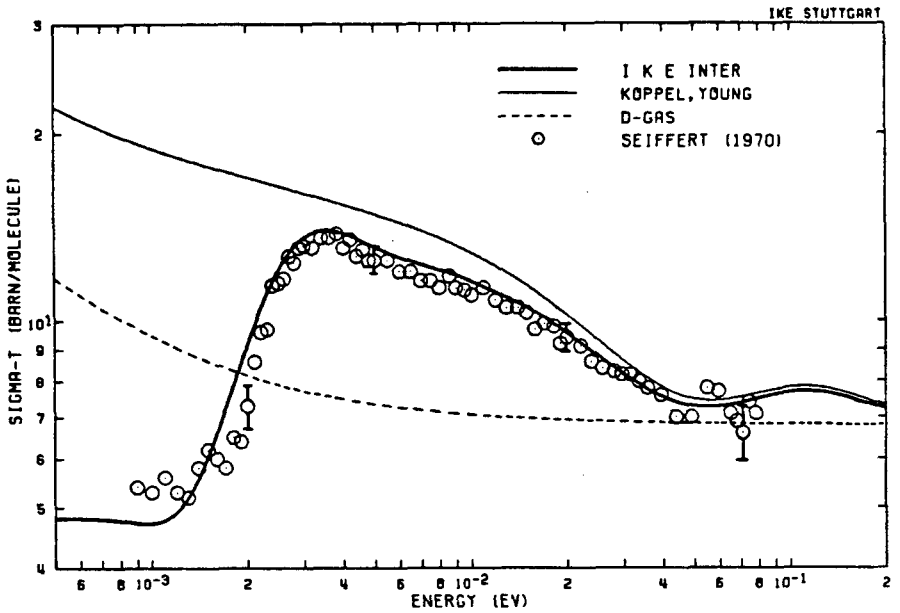

Fig. 2: Total neutron cross sections for normal-deuterium (n-D_2) at T = 19 K

For the benchmark studies multigroup cross sections for 176 energy groups in the thermal energy range are generated with a modified version of NJOY to take account for the extended scattering law data [1]. These data then are completed via CGM for the epithermal and fast neutron energy range. The benchmark calculations are done for 102 energy groups with the transport code ANISN both for H_2 (Fig. 3) and D_2 (Fig. 4). It is clearly seen that the commonly used Koppel-Young-theory [2] for n - H_2 overestimates the cold neutron fluxes, whereas for n - D_2 because of the missing intermolecular interaction it underestimates the cold neutron flux.

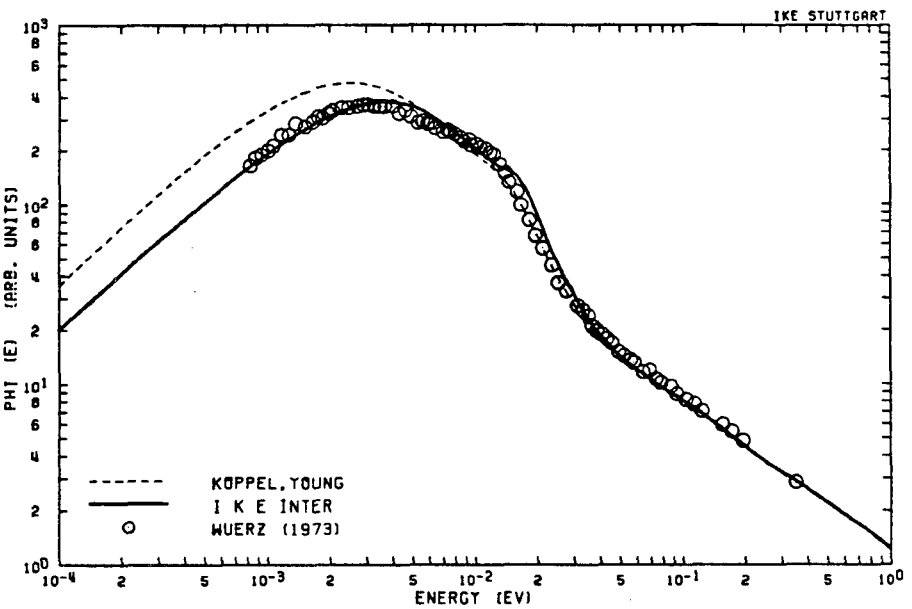

Fig. 3: Neutron leakage spectrum of a liquid hydrogen cold neutron source (32,8 % p - H_2) at T = 20 K

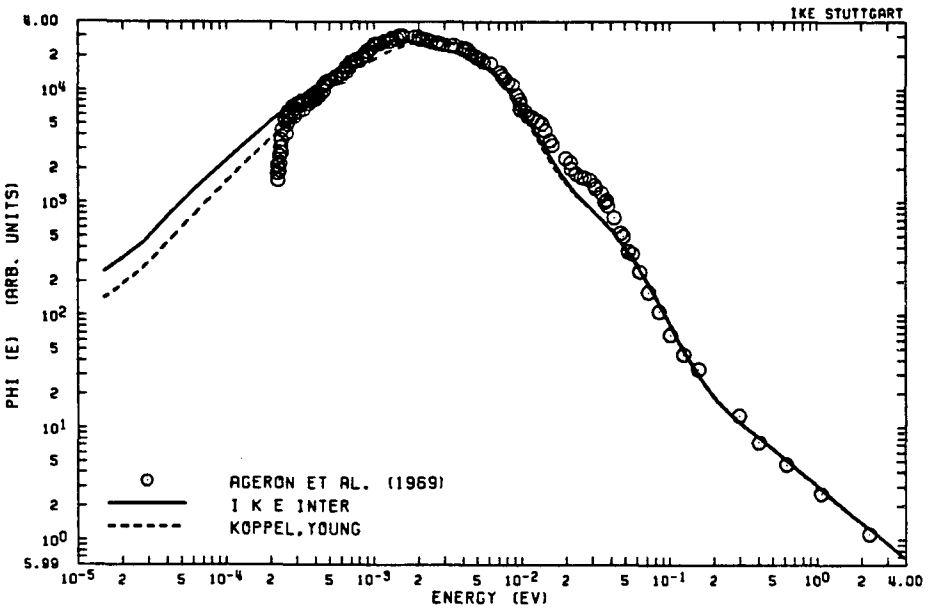

Fig. 4: Neutron leakage spectrum of a liquid deuterium cold neutron source ($n - D_2$) at $T = 23$ K

References

[1] Bernnat, W.; Emendörfer, D.; Keinert, J.; Mattes, M.: Flüssigkeitsmodelle für die Neutronenstreuung an Wasserstoff und Deuterium unter Berücksichtigung der innermolekularen und zwischenmolekularen Interferenz. Stuttgart: IKE, 1989 (IKE 6-175)

[2] Young, J.A.; Koppel, J.U.: Slow Neutron Scattering by Molecular Hydrogen and Deuterium. Phys. Rev. 135, A603 (1964)

[3] Würz, H.: Untersuchungen zur Neutronenthermalisierung an flüssigem Ortho- und Para-Wasserstoff. Karlsruhe: 1973 (KFK-1697)

[4] Ageron, P.; De Beaucourt, Ph.; Harig, H.D.; Lacaze, A.; Livolant, M.: Experimental and Theoretical Study of Cold Neutron Sources of Liquid Hydrogen and Liquid Deuterium. Cryogenics 9 (1969), 42

2. Pre-equilibrium Model Calculations with ALICE

M. Mattes, A. Sohn

Medium energy nuclear are needed for many applications, however the upper limit of existing evaluated neutron data files is 20 MeV.

For the prediction of neutron-induced reaction cross sections, particle emission spectra and angular distributions for higher neutron energies we are testing, updating and modifying the pre-equilibrium model code ALICE/ALISO [1] as we need a program that we can use with some confidence to predict cross-sections of reactions that have not been measured and perhaps cannot be measured. Furthermore, it is desirable for these calculations to be as simple as possible, so that a large number of cross-sections may be obtained in a short time. More specifically, we want to know how reliably ALICE can give us the cross-sections we need, without arbitrary variations of parameters. It is not always easy to assess this from published papers since the extent of parameter variation that was needed to obtain the fits shown is not always clear.

It turned out that the possibility to override internally determined input values and calculational parameters requires detail checks and further programming as well as for the output of all necessary data to store in ENDF-6 format.

Examples of our results are shown in figures 1 to 3 in comparison with measurements. For elements the calculation was done for the individual isotopes taking into account the natural abundances.

References:

[1] M. Blann, J. Bisplinghoff: Code ALICE/Livermore 82. UCID-19614 (1982) and update UCID-20169 (1985)

[2] A. Pavlik, H. Vonach: Evaluation of the angle integrated neutron emission cross sections from the interaction of 14 MeV neutrons with medium and heavy nuclei. Physik Daten/Physics Data No. 13-4 (1988)

[3] H.K. Vonach, P. Nagel: Blind intercomparison for n+^{184}W at 25.7 MeV. Newsletter of the NEA Data Bank No. 34 (1989), NEANDC-253"U", INDC(NEA)7

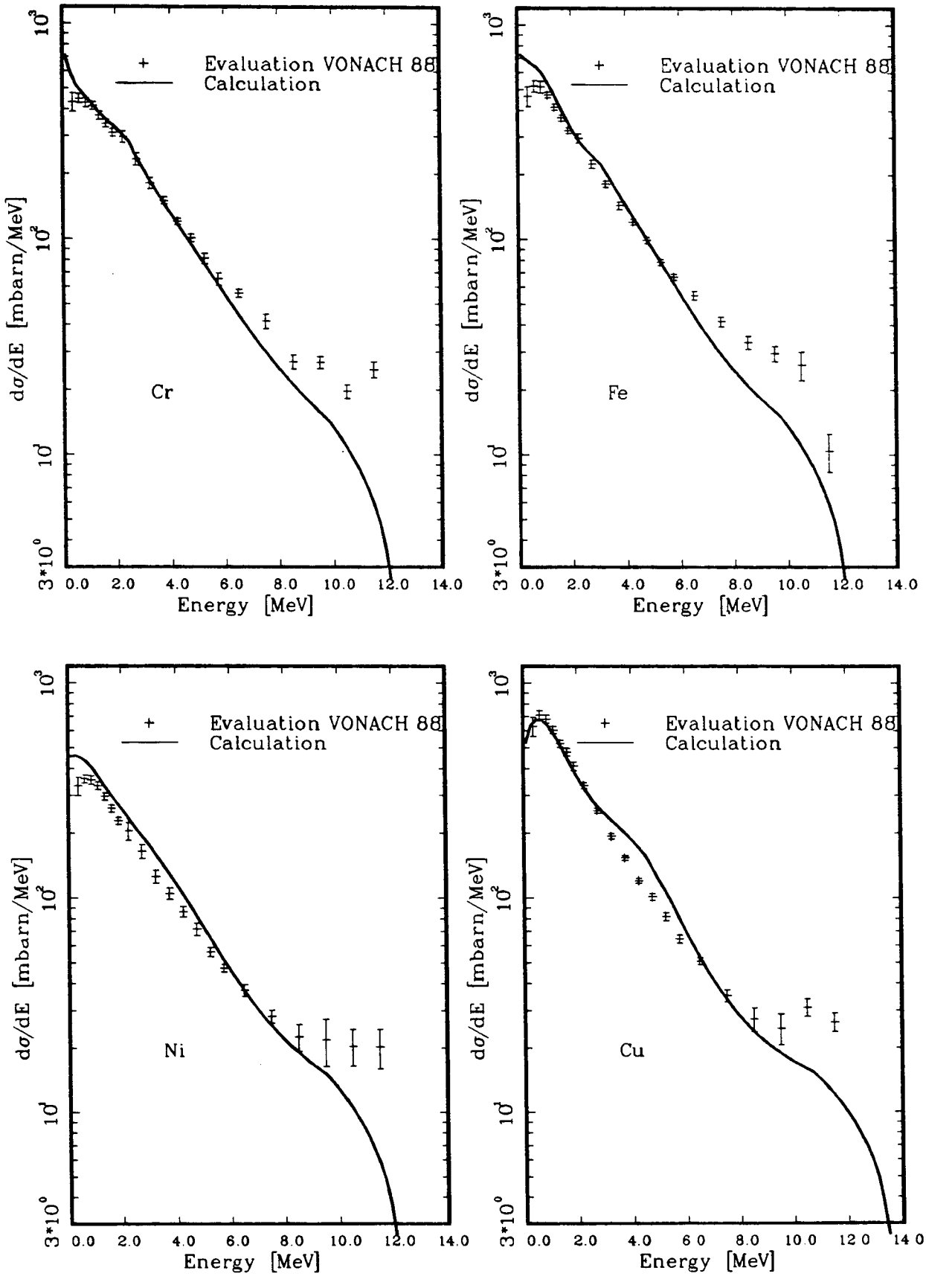

Fig. 1: Calculated neutron emission cross sections for incident neutron energy of 14.1 MeV for Cr, Fe, Ni and Cu in comparison with evaluated data by Vonach [2] .

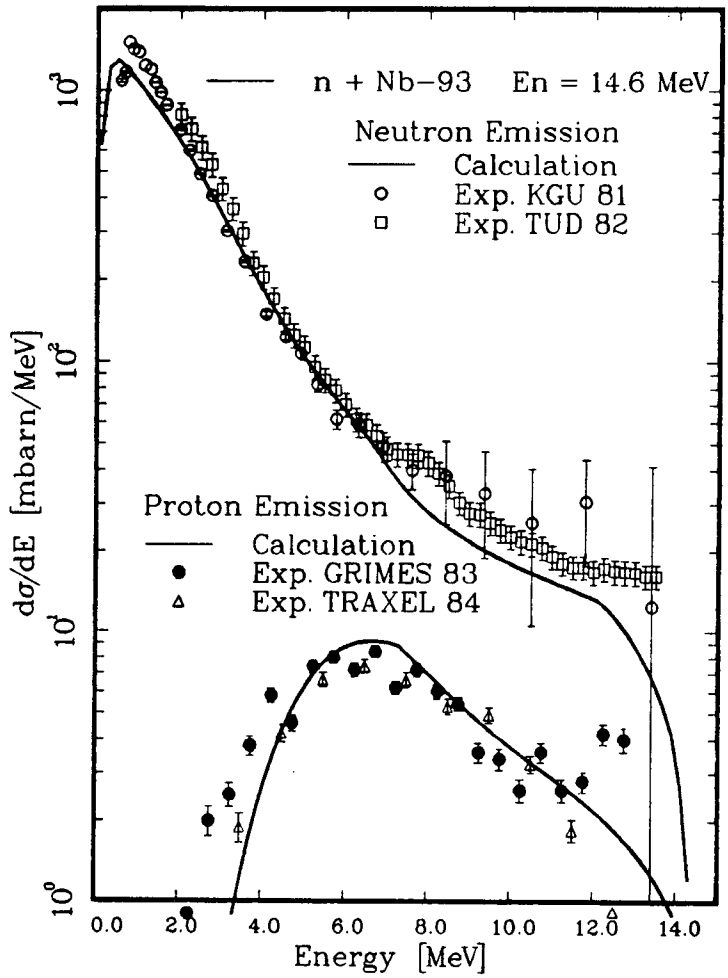

Fig. 2: Neutron and proton emission spectra for 14.6 MeV incident neutrons.

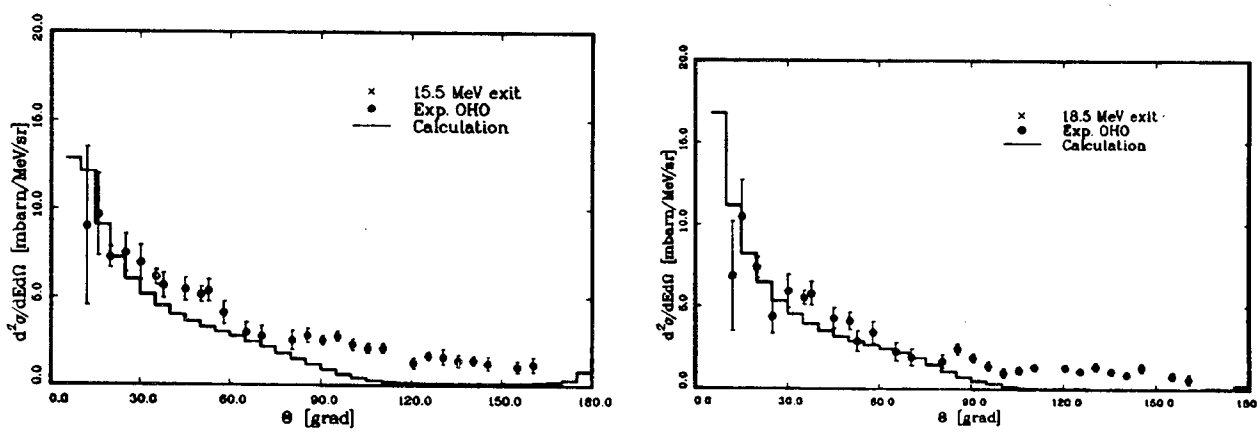

Fig. 3: Double differential neutron cross sections for ^{184}W for incident neutron energy of 25.7 MeV for several secondary neutron energies; experimental data given in [3] .

3. Thermal Neutron Scattering Law Data in ENDF-6 Format

M. Mattes

The ENDF-6 format now allows to store in addition to the thermal scattering data $S(\alpha,\beta)$ the effective temperature T_{eff}, Debye-Waller coefficients and data associated with coherent elastic scattering. All these data are required to obtain the total scattering cross section in the thermal energy range. File 7 is now complete in itself.

We translated $S(\alpha,\beta)$ for hydrogen bound in H_2O into this extented format and checked the processing with NJOY [1]. The necessary changes in this nuclear data processing system are done and will be included in the version NJOY-89.0 to be presented at the Seminar-Workshop on NJOY and THEMIS to be held in June 1989 at the NEA Data Bank, Saclay.

The transformation of $S(\alpha,\beta)$ for further moderator materials into ENDF-6 format will be done for JEF-2.

References:

[1] R.E.MacFarlane, D.W. Muir, R.M. Boicourt: The NJOY Nuclear Data Processing System. LA-9303-M (ENDF-324), Vol.I, II, III, IV (1982-1985)

PHYSIKALISCH-TECHNISCHE BUNDESANSTALT
BRAUNSCHWEIG

1. Neutron Data

1.1 Cross Section for the $^{27}Al(n,\alpha)$ and $^{24}Mg(n,p)$ Reactions

G. Börker, H. Klein, W. Mannhart, M. Wagner*, G. Winkler*

The analysis of this experiment has been completed. Data between 8.3 MeV and 14.8 MeV were determined relative to the $^{238}U(n,f)$ cross section. First results have been presented elsewhere [1]. The experimental results for $^{27}Al(n,\alpha)$ are shown in Fig. 1 and compared with the ENDF/B-V data. In the data analysis a possible bias factor due to the fission deposit mass determination has been detected. Further investigations of this are in progress. The final numerical data will be released as soon as this common normalization factor is fixed.

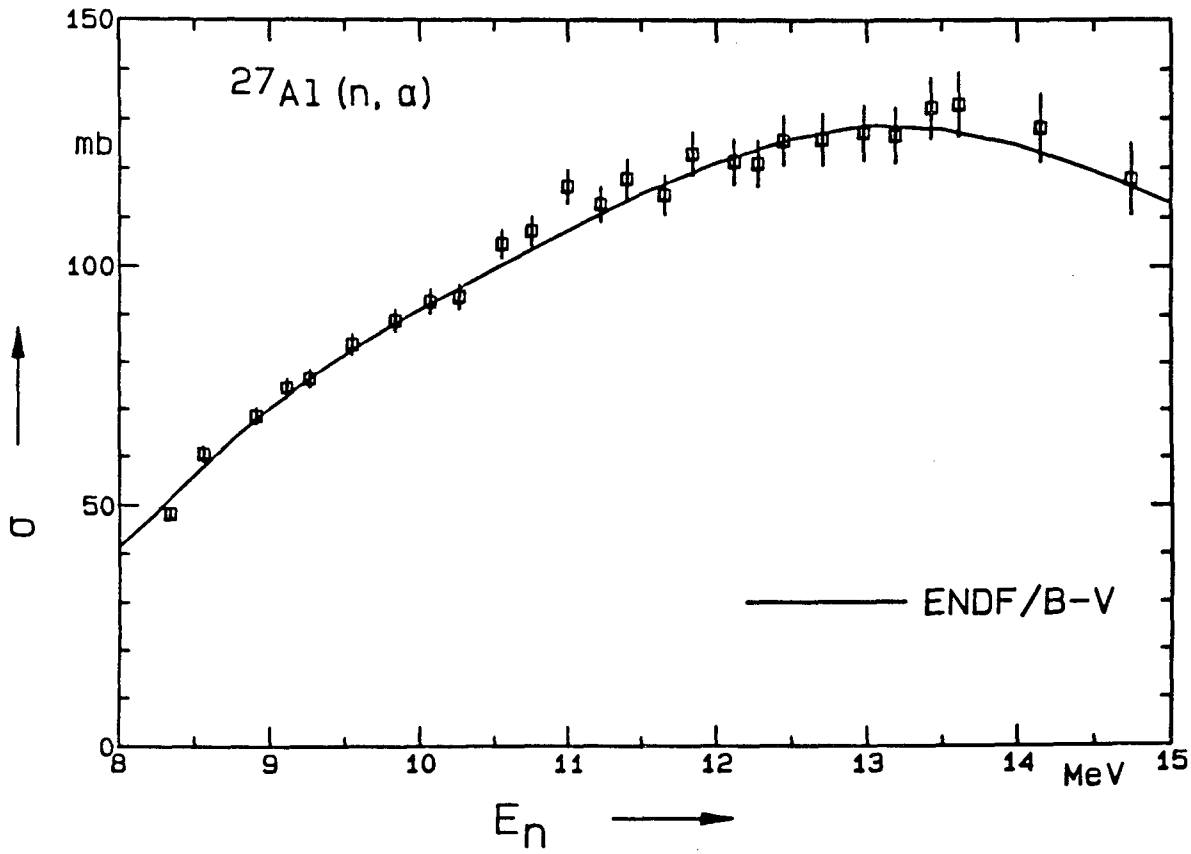

Fig. 1: Experimental cross section for $^{27}Al(n,\alpha)$ in comparison with ENDF/B-V

*Institut für Radiumforschung und Kernphysik, Wien

1.2 Measurement of the $^{54}Fe(n,\alpha)^{51}Cr$ Cross Section

W. Mannhart, G. Börker, G. Müller

The data base available for this cross section is sparse. Experimental data between 9.2 MeV and 14.8 MeV (in steps of approximately 0.5 MeV) were determined by using the D(d,n) reaction for neutron production. All measurements were performed relative to the $^{27}Al(n,\alpha)$ cross section. This experiment extends the energy range covered by a similar previous experiment [2] to higher neutron energies. The data analysis is in progress.

1.3 Reaction Cross Sections on Carbon for Energies from 11.5 MeV to 19 MeV

B. Antolkovic*, G. Dietze, H. Klein

Neutron-induced reaction cross sections were measured for carbon in the energy range from 11.5 MeV to 19 MeV.

Response functions of an NE213 scintillation detector were measured in steps of at least 0.5 MeV for monoenergetic neutrons, applying suitable time-of-flight techniques and comparing them with Monte Carlo simulations. The total cross section of all reactions with charged particles (except carbon recoils) in the exit channel was determined with respect to the n-p scattering cross section (Fig. 2). The data from preliminary results [3] had to be reduced by up to 12.4 % between 12.8 MeV and 19 MeV due to an improved analysis.

In addition, the $^{12}C(n,n'3\alpha)$ reaction was investigated for neutron energies of 11.9, 12.9, 14.0, 14.8, 17.0 and 19.0 MeV using the nuclear emulsion technique. Because all α-particles are registered for each event, this kinematically complete measurement results in total (Fig. 3) and partial cross sections for the various channels of the $^{12}C(n,n'3\alpha)$ reaction.

The experimental data presented show deviations of up to ± 25 % from ENDF/B-V [4] recommendations, while the evaluation recently performed by E. Axton [5] is partially confirmed. Reasonable agreement is found with most of the recent scattering experiments, thus this data set represents a valuable basis for further evaluations. The analysis performed has, however, shown that additional data for some partial reaction cross sections are urgently needed. In particular, experimental data on the inelastic scattering via the 7.63 MeV level

*Ruder Boskovic Institute, Zagreb, Yugoslavia

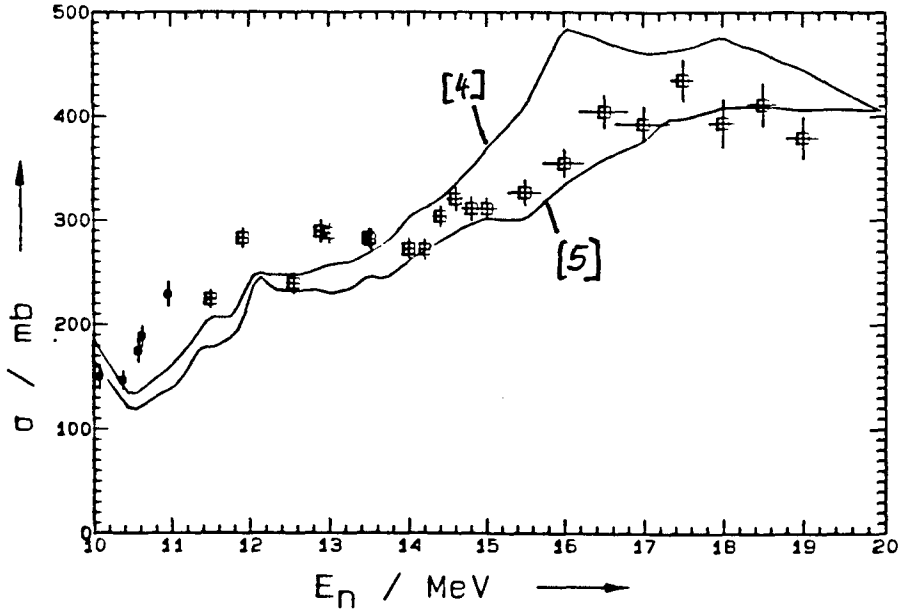

Fig. 2: Total reaction cross section of neutron induced reactions on carbon except those via the 7.65 MeV state of ^{12}C. Experimental data measured with a liquid scintillator are compared with evaluations namely ENDF/B-V [4] and recent results of E. J. Axton [5].

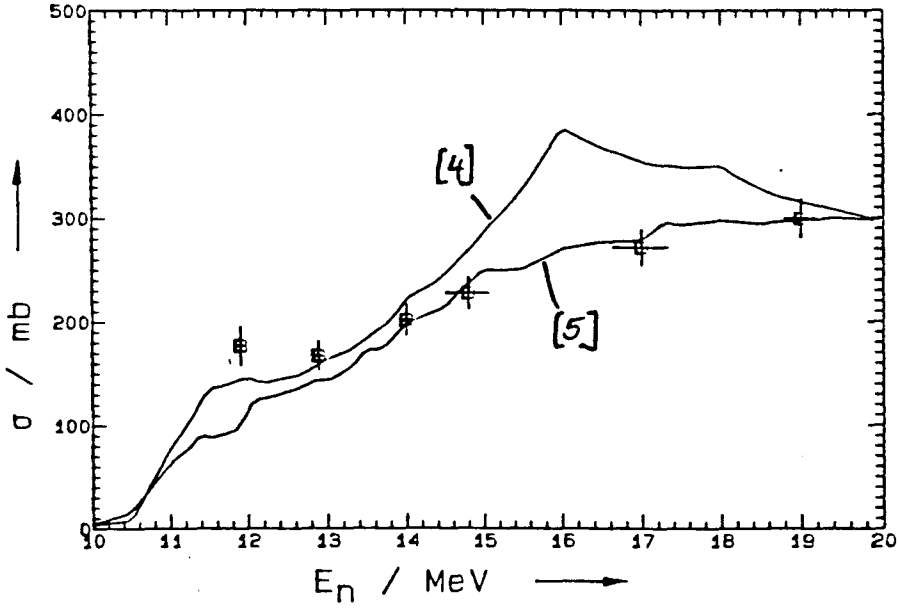

Fig. 3: Cross section of the $^{12}C(n,n'3\alpha)$ breakup reaction also with the exception of the transition via the 7.65. Experimental data measured with nuclear emulsions are compared with ENDF/B-V [4] and Axton's recent evaluations [5].

of ^{12}C, at least an estimate of the upper limit for neutron energies from the threshold up to 14 MeV, and the differential cross section of the $^{12}C(n,\alpha_0)$ reaction for the entire energy range are required.

1.4 Measurement of Neutron Kerma Factors

H.J. Brede, P. Dahmen*, H.G. Menzel*, P. Pihet*, U.J. Schrewe and H. Schuhmacher

Low-pressure proportional counters have been used to determine neutron kerma factors for various materials [6, 7, 8]. The kerma factor, k_Φ, - a basic quantity in neutron dosimetry - is defined as

$$k_\Phi = K / \Phi = \sum_l N_l \sum_j E_{lj} \sigma_{lj}$$

where K is the neutron kerma, Φ the neutron fluence, N_l the number of target nuclides of type l per unit mass in the material, E_{lj} the average energy transferred to the kinetic energy of charged particles in interactions of type j, and σ_{lj} the respective cross section. Measurements with monoenergetic neutrons between 14 and 19 MeV have revealed discrepancies with evaluated cross section data for carbon as given by ENDF/B-V [7].

The investigations have been extended to monoenergetic neutrons with energies between 20 and 60 MeV. Particular effort is required to separate low-energy neutron components present in the radiation fields. A multi-parameter data acquisition system specifically designed for time-of-flight measurements with low-pressure proportional counters was developed and tested at the accelerator facility of the PTB [9]. Figure 4 shows the frequency of events as a function of pulse height and the time of flight, measured with a proportional counter the walls of which were made of tissue-equivalent plastic (A-150). Prompt photons and neutrons produced in the target are clearly separated.

For the measurements performed recently at the Paul-Scherrer Institute, Villigen, Switzerland, proportional counters with walls made of A-150, carbon, aluminium and iron were used in beams of nearly monoenergetic neutrons of 27.1 and 39.7 MeV. The neutron fluence was determined with a proton recoil telescope

*Universität des Saarlandes, Homburg/Saar

consisting of a polyethylene radiator, two proportional counters and two surface barrier detectors. The analysis of the measurements is in progress.

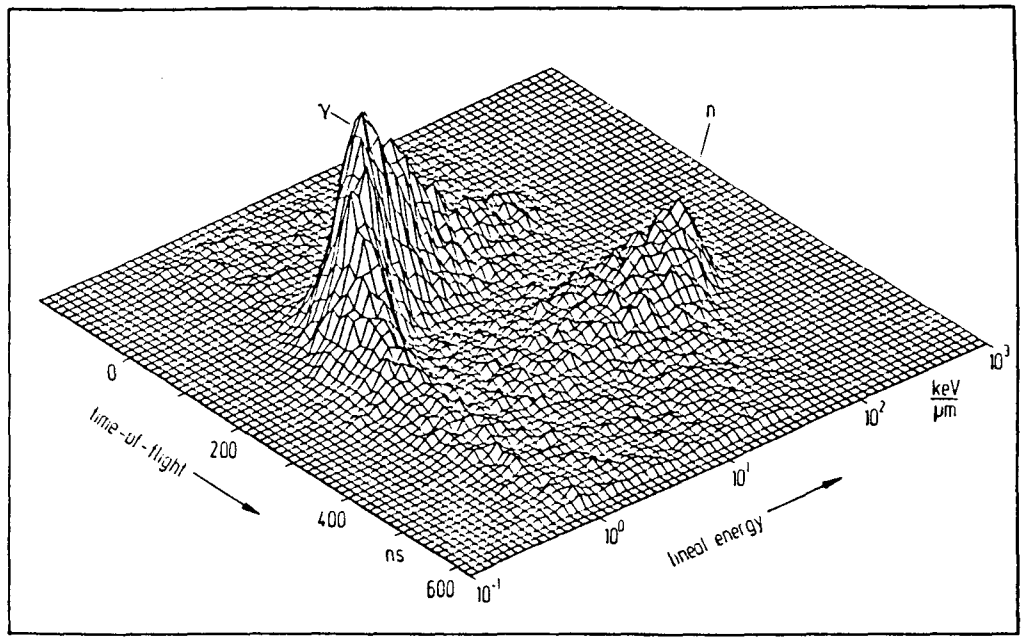

Fig. 4: Frequency of events as a function of lineal energy (defined as the ratio of energy deposited in the cavity of the proportional counter and the mean chord length of the cavity) and of the time of flight, measured with a tissue-equivalent proportional counter. Neutron energy: 70 keV, distance from target: 50 cm.

2. Radionuclide Data

2.1 Photon Emission Probabilities

U. Schötzig

Gamma and X-ray emission probabilities of several nuclides were determined by using sources of known activity, and efficiency calibrated Ge(Li), HPGe and Si(Li) spectrometers. The results are summarized in Table 1. Uncertainties (in parentheses) correspond to one standard deviation.

Table 1: Photon emission probabilities p

Nuclide	Energy in keV	Radiation	p
^{65}Zn	511.0	Annihilation	0.0284(4)
	1115.5		0.502(4)
^{88}Y	898.04		0.942(9)
^{89}Sr	909.2		$9.61(13)10^{-5}$
^{147}Pm	39.2	Sm-$K_{\alpha 2}$	$2.23(16)\cdot 10^{-5}$
	40.1	Sm-$K_{\alpha 1}$	$4.29(14)\cdot 10^{-5}$
	45.4	Sm-$K_{\beta 1}$'	$1.32(5)\cdot 10^{-5}$
	46.6	Sm-$K_{\beta 2}$'	$0.385(13)\cdot 10^{-5}$
	121.2		$2.65(6)\cdot 10^{-5}$
^{204}Tl	68.9	Hg-$K_{\alpha 2}$	0.00474(20)
	70.8	Hg-$K_{\alpha 1}$	0.00812(34)
	80.1	Hg-$K_{\beta 1}$'	0.00273(10)
	82.5	Hg-$K_{\beta 2}$'	0.00081(3)
	72.8	Pb-$K_{\alpha 2}$	$4.4(3)\cdot 10^{-5}$
	75.0	Pb-$K_{\alpha 1}$	$6.1(3)\cdot 10^{-5}$
	84.8	Pb-$K_{\beta 1}$'	$2.7(2)\cdot 10^{-5}$
	87.3	Pb-$K_{\beta 2}$'	$7.3(2)\cdot 10^{-6}$
^{210}Pb	9.42	Bi-L_l	0.0055(3)
	10.80	Bi-L_α	0.0948(17)
	11.68	Bi-L_η	0.00075(4)
	12.6	Bi-$L_{\beta 4,6}$	0.0255(7)
	13.0	Bi-$L_{\beta 1,2,15}$	0.0659(33)
	13.3	Bi-$L_{\beta 3,5}$	0.0154(9)
	13.6	Bi-$L_{\beta 10}$	0.0023(1)
	15.2	Bi-$L_{\gamma 1}$	0.00682(27)
	15.6	Bi-$L_{\gamma 2}$	0.0138(4)
	16.2	Bi-$L_{\gamma 4}$	0.0030(2)
	46.5		0.0424(5)
^{44}Ti	67.85		0.935(15)
	78.38		0.974(13)
	146.23		0.00093(3)
^{44}Sc	511.0	Annihilation	1.88(3)
	1499.5		0.00912(15)
	2656.4		0.00115(6)

References

[1] G. Börker, H. Klein, W. Mannhart, M. Wagner, G. Winkler: in "Nuclear Data for Science and Technology" (S. Igarasi, Ed.), Saikon Publ. Company, Tokyo (1988) 1025

[2] D. L. Smith, J. W. Meadows, L. R. Greenwood, W. Mannhart, L. P. Geraldo: "Reports to the DOE Nuclear Data Committee", NEANDC(US)-226/U (1988) 6

[3] B. Antolkovic, G. Dietze, H. Klein: in: "Fast Neutron Physics", (D. Miljanic et al., Eds.) Ruder Boskovic Inst., Zagreb (1986) 137

[4] Evaluated Nuclear Data File, ENDF/B-V, Brookhaven National Laboratory, New York (1979)

[5] E. J. Axton, private communication (1987)

[6] H.G.Menzel, G.Bühler, H.Schuhmacher, H.Muth, G.Dietze and S.Guldbakke: Phys. Med. Biol. 29 (1984) 1537

[7] G.Bühler, H.G.Menzel, H.Schuhmacher and G.Dietze: Radiat. Prot. Dosim. 13 (1985) 13

[8] G.Bühler, H.G.Menzel, H.Schuhmacher, G.Dietze and S.Guldbakke: Phys. Med. Biol. 31 (1986) 601

[9] U.J.Schrewe, H.J.Brede and G.Dietze: "Dosimetry in mixed neutron-photon fields with tissue-equivalent proportional counters"., Radiat. Prot. Dosim., in press

FACHINFORMATIONSZENTRUM KARLSRUHE

Status Report

H. Behrens, H.-W. Müller

1. Evaluated Nuclear Structure and Decay Data

Nuclear structure and decay data are evaluated by an international network of evaluation centers under the auspices of the International Atomic Energy Agency (IAEA).
The FACHINFORMATIONSZENTRUM KARLSRUHE (FIZ) was in charge of the evaluation of the mass range A = 81 - 100. The evaluations are published as "Nuclear Data Sheets". The computerized version is the Evaluated Nuclear Structure Data File (ENSDF) which covers the mass range A = 1 - 263. A special representation of radioactivity data for application purposes is the file MEDLIST. Data from both files can be retrieved either online or on request from the Fachinformationszentrum (FIZ).

Updates of ENSDF:

ENSDF and MEDLIST were updated in June and October. 36 mass chains have been re-evaluated in 1988.

Current contents:

ENSDF: 2,434 nuclides
10,448 data sets (each representing a special type of experiment, or ADOPTED LEVELS, GAMMAS properties)

822,673 records (of 80 byte)

MEDLIST: 2,307 data sets (each representing one decay mode of a radionucleus)

94,692 records

Status of mass chain evaluations of FIZ (A = 81 -100) from 1.4.88 to 31.3.89:

A = 86	published
A = 84	finished, in print
A = 89	finished, in review
A = 85, 87, 91	in progress

References

Nuclear Data Sheets for A=86
H.-W. Müller, J.W. Tepel
Nuclear Data Sheets 54 (1988), 527

Nuclear Data Sheets for A=84
H.-W. Müller
Nuclear Data Sheets 56 (1989), 551

2. Database GAMCAT

The database GAMCAT comprises the computerized versions of the "Catalog of Gamma Rays from Radioactive Decay" by U. Reus and W. Westmeier (At. Data Nucl. Data Tables 29, 1 and 29, 193 (1983)) and the "Catalog of Alpha Particles from Radioactive Decay" by W. Westmeier and A. Merklin (Physics Data 29-1 (1985)). A Personal Computer Version has been created and will be available soon. In this system access is possible either by parent nucleus or by gamma ray or alpha particle energy.
The database will be distributed together with the retrieval system on two 5 1/4" HD floppy disks. For the installation, an AT compatible computer is required with a hard disk and 640 K memory, running under DOS 2.11 or later. Approx. 2 MB storage space is needed on the hard disk.

Contents:

2,326 radionuclei
47,000 gamma rays
1,900 alpha particle branches

APPENDIX

Addresses of Contributing Laboratories

Institut für Kernphysik III
Director: Prof. Dr. G. Schatz
Senior reporter: Dr. F. Käppeler
Kernforschungszentrum Karlsruhe
Postfach 3640
7500 Karlsruhe

Institut für Material- und Festkörperforschung
Director: Dr. K. Anderko
Senior reporter: Dr. S. Cierjacks
Kernforschungszentrum Karlsruhe
Postfach 3640
7500 Karlsruhe

Institut für Neutronenphysik und Reaktortechnik
Director: Prof. Dr. G. Kessler
Senior reporter: Dr. F. Fröhner
Kernforschungszentrum Karlsruhe
Postfach 3640
7500 Karlsruhe

Institut für Chemie (1): Nuklearchemie
Director: Prof. Dr. G. Stöcklin
Senior reporter: Dr. S.M. Qaim
Kernforschungsanlage Jülich
Postfach 1913
5170 Jülich

Institut für Kernphysik
Arbeitsgruppe Strahlungstransport
Head and senior reporter: Dr. D. Filges
Kernforschungsanlage Jülich
Postfach 1913
5170 Jülich

Institut für Physik
Director: Prof. Dr. W. Michaelis
Senior reporter: Dr. R. Pepelnik
GKSS-Forschungszentrum Geesthacht GMBH
Postfach 1160
2054 Geesthacht

Zentraleinrichtung für Strahlenschutz
Head and senior reporter: Prof. Dr. H. Michel
Universität Hannover
Am Kleinen Felde 30
3000 Hannover 1

Abteilung Nuklearchemie
Director: Prof. Dr. G. Stöcklin
Senior reporter: Dr. U. Herpers
Universität zu Köln
Zülpicher Str. 47
5000 Köln 1

Institut für Kernchemie
Director: Prof. Dr. G. Herrmann
Senior reporter: Prof. Dr. H.O. Denschlag
Universität Mainz
Fritz -Strassmann-Weg 2
6500 Mainz

Fachbereich Physik der
Technischen Universität München
Abteilung E14, Forschungsreaktor
Senior reporter: Dr. W. Waschkowski
8046 Garching/München

Institut für Kernenergetik und Energiesysteme
Director: Prof. Dr. A. Schatz
Senior reporter: DP M. Mattes
Universität Stuttgart
Almandring 3
7000 Stuttgart 80

Physikalisch-Technische Bundesanstalt
Abteilung 6, Atomphysik
Director: Prof. Dr. S. Wagner
Bundesallee 100
3300 Braunschweig

Fachinformationszentrum Energie, Physik, Mathematik
Directors: Dr. W. Rittberger, E.-O. Schulze
Senior reporter: Dr. H. Behrens
Kernforschungszentrum
7514 Eggenstein-Leopoldshafen